DESIGN AND CONSTRUCTION OF A SWITCH MODE CONSTANT VOLTAGE BATTERY CHARGER FOR NEW GENERATION MOTOR VEHICLES

BY

OSINOWO, Olusegun Emmanuel

M.ENG/SEET/2008/2086

THESIS SUBMITTED TO THE POSTGRADUATE SCHOOL, FEDERAL UNIVERSITY OF TECHNOLOGY MINNA, NIGERIA IN PARTIAL FULFILLMENT OF THE REQUIREMENT FOR THE AWARD OF THE DEGREE OF MASTER OF ENGINEERING (M.ENG) ELECTRICAL AND ELECTRONICS ENGINEERING (ELECTRICAL POWER AND MACHINES OPTION)

APRIL, 2012

DECLARATION

I hereby declare that this thesis titled: Design and Construction of a Switch Mode Constant Voltage Battery Charger for New Generation Motor Vehicle, is a collection of my original research work and it has not been presented for any other qualification anywhere. Information from other sources (published or unpublished) has been duly acknowledged.

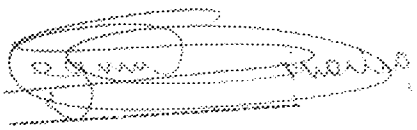

SIGNATURE & DATE

OSINOWO, Olasegun Emmanuel
M.ENG/SEET/2008/2086
FEDERAL UNIVERSITY OF TECHNOLOGY,
MINNA, NIGERIA

CERTIFICATION

The thesis titled: "Design and Construction of A Switch Mode Constant Voltage Battery Charger for New Generation Motor Vehicles" by: Osinowo, Olusegun Emmanuel (M.Eng/SEET/2008/2086) meets the regulations governing the award of the degree of Master of Engineering (M.Eng) of the Federal University of Technology, Minna and it is approved for its contribution to scientific knowledge and literary presentation.

Engr. A.G. Raji
SUPERVISOR

Signature & Date (May 25, 2012)

Engr. A.G. Raji
HEAD OF DEPARTMENT

Signature & Date (May 25, 2012)

Prof. M.S. Abolarin
DEAN, SEET

Signature & Date 08/08/12

Prof. (Mrs.) S.N. Zubairu
DEAN, POST GRADUATE SCHOOL

Signature & Date 27/7/12

ACKNOWLEDGMENTS

This research work has been carried out between January 2010 and December 2011 in the Department of Electrical and Electronics Engineering of Federal University of Technology, Minna. Many people have helped me in the realization of this work and I would like to take this opportunity to express my gratitude to all of them.

I am indeed indebted to my supervisor, Engr.A. G. Raji, for his sincere belief in my ability to successfully execute this research project work. I appreciate his interest, advice and constructive criticism that led to the successful completion of this work.

I must express my profound gratitude to the Vice-Chancellor of Federal University of Technology, Minna, Professor M.S. Audu, the Dean School of Engineering, Professor M.S. Abolarin, the Dean Postgraduate School, Professor (Mrs.) S.N. Zubairu, the Head of Department of Electrical and Electronics Engineering, Engr. A. G. Raji, and all the lecturers and staff of Electrical and Electronics Engineering Department for all their contributions to the successful completion of the Master 's Degree program.

I would like to thank my colleagues Godswill, Tola, Ganiyu, Ambafi, Mr. Ogunsanwo Godwin, Mr. Ola and Engr. Mohammad Achanya for fruitful technical discussions that improved this research work. I also would like to acknowledge all the Laboratory attendants of the Electrical/Electronic Department of Federal University of Technology Minna for their valuable advice. I am grateful to Dr. M.N. Nwohu who is the postgraduate coordinator.

Financial support of my employer, Nigerian Television Authority is gratefully appreciated. I am obliged to Mr. Joshua Vincent, Mr. Isaac Efah and Mr. Joseph that did the typesetting.

Many thanks to Mr. Femi Ibrahim, Engr. Nosa Osawe, Mr Jonathan Amoo of blessed memory, Engr. Joshua Bishi, Engr.Dakahap, Engr. Babatunde and Engr. Bathlomew of Kaduna Polytechnic and any other persons not mentioned above who were either directly or indirectly involved with the success of this project and their view points.

Special thanks to my family and friends for supporting and encouraging me during the research and writing of this thesis.

ABSTRACT

This project presents the design and implementation of a reliable, cost-effective 42V battery charger, charging off board 36V batteries for the anticipated new generation motor vehicles. The choice of switching mode power supply for the design ensures that losses in the device are minimised compared with what could have obtained if a linear electronics equivalent were adopted. In this thesis AC to DC converter with SMPS circuit, having a power MOSFET for switching operation and a PWM based feedback circuit for driving the switching of the MOSFET, is designed and simulated in MULTISM circuit design environment before implementation. The line voltage at 220/50Hz is taken as input; this voltage is stepped down, rectified and passed through filter capacitor to give an unregulated DC voltage. This unregulated voltage is chopped using a MOSFET switch, driven by PWM feedback signal, to control the output voltage level. A high frequency isolation transformer is used to isolate the DC output from input supply. The transformer output is again rectified by the high frequency diode bridge rectifier and is filtered using a capacitor to give the regulated DC output of 42V. Desired features for battery charger such as low cost, fast charging, high efficiency, small in size and high reliability are fully achieved.

TABLE OF CONTENTS

		Page
Title Page		i
Declaration		ii
Certification		iii
Acknowledgements		iv
Abstract		vi
Table of Contents		vii
List of Tables		xi
List of Figures		xii
List of Plates		xiv
Abbreviations, Glossaries and Symbols		xv
CHAPTER ONE: INTRODUCTION		1
1.1	Background to the Study	1
1.2	Motivation	3
1.3	Aims and Objectives	3
1.4	Methodology	3
1.5	Scope and Limitation of work	3
1.6	Organisation of the thesis	4
CHAPTER TWO: LITERATURE REVIEW		5
2.1	Introduction	5
2.2	Power Supply Family	11
2.2.1	Linear Power Supply	11
2.2.2	SMPS Power Supply	11
2.3	Types of Battery Chargers	13

2.3.1	Linear Chargers	13
2.3.2	Switch Mode Chargers	14
2.3.3	SCR Chargers	14
2.3.4	Ferro resonant Chargers	15
2.4	Lead Acid Batteries	16
2.4.1	Discharge	17
2.4.2	C-Rate	18
2.4.3	Battery efficiency	19
2.4.4	Charging	19
CHAPTER THREE: MATERIALS AND METHOD		22
3.1	Introduction	22
3.1.1	Specifications	22
3.2	The Block Diagram Analysis	24
3.2.1	Input Rectifier 1	25
3.2.2	Filtering capacitor	29
3.2.3	Input Rectifier 2	29
3.2.4	The Power Switches Mosfet	30
3.2.5	Control Section	31
3.2.6	Oscillator	32
3.2.7	Comparator and PWM	33
3.2.8	Transformer Section	34
3.2.8.1	Design and dimensional data for ferrite cores	35
3.2.8.2	Determination of low input current	36
3.2.8.3	Determination of Primary rms current, Iprms	36
3.2.8.4	Determination of Primary turns	36

3.2.8.5	Determination of current density (J)	37
3.2.8.6	Determination of the required bare wire area	38
3.2.8.7	Determination of number of strands (NSp)	38
3.2.8.8	Determination of the primary new μΩ/cm	38
3.2.8.9	Determination of the primary winding resistance (Rp)	38
3.2.9.0	Determination of the primary copper loss (Pp)	39
3.2.9.1	Determination of the transformer secondary voltage, Vs	39
3.2.9.2	Determination of number of secondary turns (Ns)	39
3.2.9.3	Determination of the secondary rms current, Isrms	40
3.2.9.4	Determination of the secondary base wire area, Aws	40
3.2.9.5	Determination of the required number of secondary strands, NS_s	40
3.2.9.6	Determination of the secondary new mW per centimeter	40
3.2.9.7	Determination of winding resistance, Rs	41
3.2.9.8	Determination of secondary copper loss, Ps	41
3.2.9.9	Determination of the copper loss, Pcu	41
3.3	Output Rectifiers	41
3.4	Heat Sink	41
3.5	Complete circuit of 42V SMPS battery charger	44
3.6	Picture of the prototype	45
CHAPTER FOUR: RESULTS		46
4.1	Introduction	46
4.2	Construction Layout	46
4.3	Rectifier 1 with without filter capacitor	48
4.3.1	Rectifier 1 with filter capacitor	48

4.4 Rectifier 2 with fixed LM7809 regulator 49

4.4.1 Rectifier 2 with oscilloscope waveform output 50

4.5 Complete circuit simulation 51

4.6 Result Obtained 55

4.7 Project Cost Estimate 55

4.8 Reliability Assessment of the battery charger 55

4.9 Durability and Safety of the battery charger 58

CHAPTER FIVE: CONCLUSIONS AND RECOMMENDATIONS 59

5.1 Conclusion 59

5.2 Recommendations 59

REFERENCES 60

APPENDICES 63

LIST OF TABLES

Table		Page
4.1	Test Results obtained when three (12V) batteries were observed	55
4.2	Components and basic failure rate	57

LIST OF FIGURES

Figure		Page
1.1	A block diagram of a 14/42v architecture	1
2.1	A block diagram of a 14/42v on-board charging system.	5
2.2	A block diagram of a SMPS	12
2.3	A block diagram of a linear charger	13
2.4	A block diagram of a SMPS charger	14
2.5	A diagram of an SCR charger	15
2.6	A block diagram of a ferroresonant charger	15
2.7	A block diagram of a Lead Acid Battery	17
2.8	A block diagram of a positive and negative plate of a lead acid battery	18
2.9	Stages of a Lead acid battery charge	20
2.10	Graph of 12V battery versus capacity at various stages of charge and discharge	21
3.1	A block diagram of a SMPS	24
3.2	A block diagram with various stages of a SMPS	24
3.3	Showing main input rectifier 1	25
3.4	Showing equivalent circuit of figure 3.3	25
3.4a	Showing graph of Vc against time	28
3.4b	Showing graph of Ic against time	28
3.4c	Showing graph of V_c, I_c and e_s against time	28
3.5	A block diagram of a filter output	29
3.6	Showing auxillary rectifier 2	30
3.7	Showing switching operation of T_1 and T_2	31
3.8	Complete circuit diagram of control IC SG3524	32
3.9a	Comparator signals for PWM	33

3.9b Comparator signals showing T_{on} and T_{off} 34

3.10 Dimension outline for ETD ferrite core 35

3.11 Heat sinks' data sheet. 43

3.12 Complete circuit diagram of 42V SMPS battery charger 44

4.1 Rectifier 1 without filter capacitor 48

4.2 Rectifier 1 with filter capacitor 49

4.3 Simulated result obtained for rectifier 1 with filter capacitor 49

4.4 Rectifier 2 with a regulator output LM7809 50

4.5 Simulated result of rectifier 2 with LM7809 51

4.6 Showing simulation 1 of the entire circuit with Multism NI 10 52

4.7 Showing simulation 2 of the entire circuit with Multism NI 10 53

4.8 Showing simulation result of the PWM during T_{on} and T_{off} 54

LIST OF PLATES

Plate		Page
I	Picture of the prototype	45
II	Picture of the power switch IRF 450 mounted on heat sink	45
III	Input supply protection stage	46
IV	Construction stage	46
V	Testing of 3 Nos of 12V battery in series	46
VI	Testing Stage	47
VII	Testing stage	47
VIII	Mosfet IRF 450 section	47
IX	36V output terminal of the charger	47
X	Testing of 3 Nos of 12V battery connected in series to obtain 36V	47

ABBREVIATIONS AND SYMBOLS

Abbreviations

AC	Alternating Current
A/D	Analog to Digital converter
DC	Direct Current
DOD	Depth of Discharge
FC	Fuel Cell
HEV	Hybrid Electrical Vehicle
ICE	Internal Combustion Engine
IGBT	Insulated Gate Bipolar Transistor
Li-Ion	Lithium-Ion
MOSFET	Metal oxide semiconductor field effect transistor
NiCd	Nickel-Cadmium
NiMH	Nickel-Metal-Hydride
PWM	Pulse Width Modulation
SOC	State of Charge
AC	Alternating current
BJT	Bipolar junction transistor
BW	Bandwidth
CCM	Continuous conduction mode
CMOS	Complementary Metal Oxide Semiconductor
dB	Decibel
EMI	Electromagnetic interference
FET	Field effect transistor
IC	Integrated circuit

I/O	Input output
IRF460	Switch MOSFET
PWM	Pulse width modulator

Symbols

C	Capacitance
D	Average duty cycle
f_s	Switching frequency
I_o	Average output current
L	Inductance
N_1	Number of turns in the primary side of a transformer
N_2	Number of turns in the secondary side of a transformer
N	Number of switching periods
P_{in}	Average input power
P_o	Average output power
$P_{o\,(max)}$	Maximum output power
$P_{o\,(min)}$	Minimum output power
t	Time
T_s	Average switching time
u(t)	Control signal
V_c	Average capacitor voltage
$V_{control}$	Control voltage
V_{in}	Average DC input current
$V_{in\,(min)}$	Minimum DC input voltage
$V_{o\,(max)}$	Maximum DC input voltage
V_L	Average inductor voltage

V_o	Average output voltage
V_{ref}	Reference voltage
ω	Angular frequency
Φ	Flux in the core (weber)
B	Flux density (weber/m2)
A_e	Cross-section area of the core (m2)
A_w	Total window area of the core (m2)
$V_{in,\,min}$	Minimum DC input voltage (V)
$V_{in,\,max}$	Maximum DC input voltage (V)
N_p	Number of turns in the primary winding
N_s	Number of turns in the secondary winding
f_s	Operating frequency of the transformer (Hz)
$I_{in,dc}$	Average input DC current (A)
$I_{in,\,rms}$	rms input DC current (A)
J	Current density (A/m2)
η	Transformer efficiency
D_{max}	Maximum duty cycle
P_o	Output power

CHAPTER ONE

1.0 INTRODUCTION

1.1 BACKGROUND TO THE STUDY

A vast increase in automotive electronic systems, coupled with related demands on power has created an array of new engineering opportunities and challenges. The automobile is undergoing a revolution in the design of its electrical system. This is the result of increasingly sophisticated engine and body controls, as well as the introduction of new electrically controlled functions. Vehicular battery management systems continuously check the condition of the car's battery, monitoring the charge to ensure the automobile will start and have enough power to maintain critical systems. Even with the engine switched off, some systems – real – time clocks, keyless entry and security devices and vehicle control interfaces such as window switches and light switches still consume power. The aim of this thesis is to design and construct a reliable, cost-effective 42V battery charger, charging off board 36V batteries for the anticipated new generation motor vehicles.

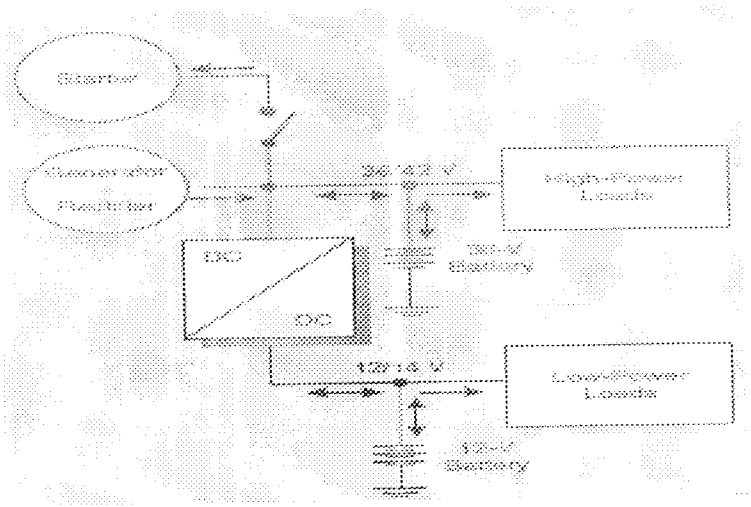

Figure 1.1: Block diagram of a 14/42V architecture (Ansoft)

In the normal motoring mode, the 12V battery supplies the starter. Once an adequate engine speed is reached, the alternator can power the loads and charge the battery. In the same way that power demand increases in the 1950s pushed the power system in vehicles from 6V to a 14V system, today the increase in the use of electronics in the vehicles is making the way for even higher voltage systems. The application of power electronics to systems that were once mechanically or hydraulically controlled, has led to a vast increase in electrical loads in the automobile. Although these advancements have increased the level of performance and reliability of automobiles, they are pushing the limits of current vehicles' power system capabilities. To meet this power, automobile manufacturers are beginning the transition to 42V system architecture.

The necessity for a dual – voltage architecture arises from the economics of transitioning all electrical systems that are currently powered at 14V to 42V. A dual – voltage bus makes use of loads that benefit from the higher voltage and maintains currently manufactured loads that operate at the lower voltage (see fig. 1.1). Loads can then be moved to the higher bus voltage as they become available Mellisa (2005).

The rationale for designing 42Volts system is as a result of the accepted principle that D.C. electricity as high as 60V is safe and does not require special materials. If the peak voltage in a system were to exceed 60V, then advanced materials and safety precautions would have to be implemented thus driving the system costs up. A 42V system would meet government regulations for safety and provide adequate power to run all current electrical applications as well as those emerging in the foreseeable future Nathan (2005).

1.2 MOTIVATION

The motivation for this project was how to design a 36V off-board battery charger in anticipation of new generation vehicles powered by 36V batteries. Presently 12V and 24V battery chargers are available commercially.

1.3 AIMS AND OBJECTIVES

The main objective of this project is to design and implement a 42V dc off board battery charger with higher-efficiency regulators using a switch mode power supply system with pulse width modulation for charge control.

1.4 METHODOLOGY

A rectifier will convert incoming ac mains into dc to provide a stable, constant voltage output with automatic current limiting. Once a battery is fully charged, the charging current has to be dissipated somehow. The result is the generation of heat and gasses both of which are bad for batteries. Elevated temperatures hasten the death of batteries and monitoring the cell temperature is a good way of detecting signs of trouble from a variety of causes. The resettable fuse was used to turn off or disconnect the charger when danger signs appear to avoid damaging the battery.

1.5 SCOPE AND LIMITATION OF WORK

The Switch mode power supply was the principle employed. The actual physics and chemical reactions in the batteries were not studied in detail.

1.6 ORGANIZATION OF THE REPORT

The remaining chapters of this project report are structured as follows: Chapter 2 deals with literature review, while chapter 3 presents materials and methods for battery charger design using mathematical evaluations; designing a control circuit using IC SG3524, building-up the simulink model of the system (converter plus controller) with Multism application software. Chapter 4 discusses the results obtained. Lastly chapter 5 deals with conclusion, summary and contribution to scientific knowledge.

CHAPTER TWO

2.0 LITERATURE REVIEW

2.1 INTRODUCTION

The time required to recharge vehicle batteries depends on the total amount of energy that can be stored in the battery, and the voltage and current (i.e., power) available from the battery charger. Battery chargers replenish the energy used by a vehicle. The battery charger converts the alternating current distributed by electric utilities into the direct current needed to recharge the battery. Battery charging may be accomplished on-board (see Fig.2.1). This project proposes an off board battery charger.

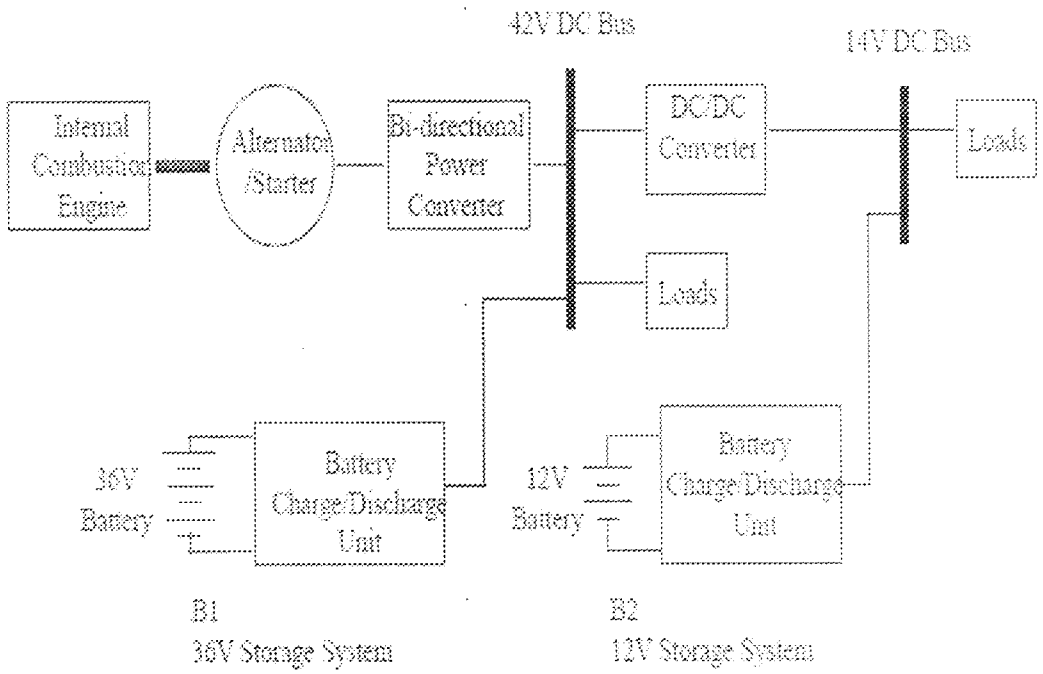

Figure 2.1: A block diagram of a 14/42V on-board charging system (Sheldon).

Introduction of an array of new electrical and electronic features into modern vehicles is generating vehicle electrical power requirements that exceed the capabilities of today's 14 volt electrical systems. In the near term (5 to 10 years), the existing 14V system will

be marginally capable of supporting the expected additional loads with escalating costs for the associated charging system. However, significant increases in vehicle functional content are expected as future requirements to meet longer-term (beyond 10 years) needs in the areas of emission control, fuel economy, safety, and passenger comfort. A higher voltage electrical system will be required to meet these future requirements. Emilian (2005).

A primary battery is one that is not rechargeable. All automotive batteries are secondary batteries Ahmed (2006). The capacity of a battery pack is measured in Ampere-hours (A – H). This unit of measure is the amount of electricity delivered at one ampere over one hour, and a capacity defined as such indicates the amount of charge that can be drawn for some length of time before the battery is considered discharged. The life of a battery is measured in cycles or years. Charging can take place at home or in a parking place if a socket is available.

Dell *et al* (2000), studied methods of evaluating 36/42V volt automotive electrical systems, this study proposed a new life test that can be performed on 42/14V electrical system in terms of its expected duty cycle and its total power capability.

Roznov (1988) studied the LM2575-ADJ step down converter and the MC33341 regulator control circuit used in the battery charger applications and offered a solution which was simple, highly efficient and cost effective. He came out with two current sources for battery chargers that can operate directly from both 12V and 24V board voltages with no change of the electrical connection.

Lidak (1996) studied the AC-DC battery charger (constant current with voltage limit) using the MC33364 and the MC33341. This study recommended that using MC33341 on the primary side (operating in the critical conduction current mode) and the MC33341 on the secondary side (controlling the output voltage and the output current) is the most reliable way for designing a dc battery charger.

Sangtaek *et al* (2008) analysed bi-directional DC/DC converters for plug-in hybrid electric vehicle (PHEV) applications. He stated that Power electronic DC to DC converters in plug-in hybrid and electric automotive applications demand high power bidirectional power flow capability, with wide input voltage range.

Output voltage of energy storage devices like ultra capacitor or battery varies with the change in load. The converter needs to provide a successful voltage regulation on the load side for a wide range of input voltage. An isolated half bridge converter was proposed in the project, with bidirectional power flow and minimum peak current for wide input voltage range through duty cycle and phase shift control. The proposed converter had competitive total device rating compared with the conventional isolated bidirectional power converters. The converter used the transformer leakage inductance as the primary energy transfer element.

Fanghua *et al* (2004) studied bi- directional forward – flyback dc- dc converter. The paper proposed a novel type of bidirectional dc-dc converter topology-forward-flyback bi directional dc-dc converter. The converter merits were as follows: The spike on the switches was much smaller than the current-fed type converter, the energy that caused the spike was much smaller than that in the current-fed converter; The current of one

side of the bi-directional dc-dc converter was continuous, the current ripple was small; There was no start-up problem in the forward-flyback bidirectional dc-dc converter; It was easy to realize soft switching; and the hybrid structure of forward and flyback converter made it suitable for high power situations. The paper analyzed the steady state operation principles in detail. The experimental results validated the analysis. Based on the principle of active clamp forward-flyback bi-directional dc-dc converter, a family of bi-directional dc-dc converters was proposed.

Bhim *et al* (2009) presented a paper on flyback technology in power conversion aimed at increasing efficiency and power density, reducing cost and using minimum components in AC-DC conversion. The proposed converter provided these features for square waveforms and constant frequency PWM. It was designed to operate in a wide input voltage range of 75-265VAC RMS with two output voltages of 5V and 20V respectively and full load output power of 5W. The proposed converter was suitable for high efficiency and high power density applications such as LCDs, TV power modules, AC adapters, motor control, appliance control, telecom and networking products.

Ondrej *et al* (1997) presented a paper on two designs of low cost current sources for battery charger applications based on the LM2575–ADJ switching step-down converter and the MC33341 regulator control circuit. The design was a highly cost effective 1.0 A current source for battery chargers with a rectangular constant–current, constant–voltage charging characteristic. This feature assured a basic protection against overcharge whose results could range from minor damage to catastrophic failure of the whole system. That circuit was designed to implement additional charge control based either on the microcontroller or on any other charging control unit in the system that operated

from NiCd or NiMH batteries. The MC33341 and this board might be used in a wide variety of applications. All functions needed were performed by just two integrated circuits and a small number of external components. That allowed a very compact printed circuit board design and a very cost effective solution. The LM2575–ADJ Easy SwitchE step down converter allowed the system to operate from 8.0 to 40 Vdc, thus allowing direct operation from both 12 and 24 V board voltages used in the automotive industry. In comparison with linear topologies of battery chargers, this circuit provided much better efficiency, especially over a wide input voltage range.

Randyll (2005) considered Photovoltaic Power Converter (PVPC) technology, developed by Atira Technologies, and its prospects for military and space applications. The research validated the hypothesis that PVPC technology enabled solar power system to produce usable power during low- and no-light conditions which standard solar power systems failed to provide. Solar cell panels were exposed to sunlight at different angles and with variable intensity, therefore the resulting output power varied depending on the illumination angle as well as the light intensity of each panel. Atira Technologies devised a novel buck-boost converter that was specifically designed to track the maximum power point of each solar panel. That would provide a significant increase in the overall available power by utilizing a switching topology in a subdued lighting condition. Although a small amount of power was generated, given enough time, a battery would reach its full charge, compared to no additional charging if the battery were using a panel without the circuit.

Melissa (2005) proposed a new tool to analyze and design military vehicle platforms: the Advanced Mobile Integrated Power System (AMPS). This tool was useful for

design and design verification of military vehicles due to its unique incorporation of mission-specific functionality. It allowed the user ease of design with the ability to customize the vehicle power system architecture and components, while permitting full control over source and load input parameters. Simulation of programmed mission sequences allowed the user to ensure that the chosen vehicle architecture could provide all of the electrical power and energy needed to support.

Consoli *et al* (2004) presented a multiphase bilateral dc/dc converter aimed to equip next-generation car having a 42-/14-V dual-voltage electric power system. In the considered automotive application, transient response was not critical because batteries were available on both sides of the converter to buffer transients. The most important considerations were cost, efficiency, and size implications in topology and magnetic components optimization. The proposed solution has been compared with a conventional single-switch converter. Experimental results showed that the proposed solution had greater efficiency over the entire input voltage range. Compactness of the power conversion system was also increased compared to conventional solutions, while the reliability was improved.

Muhammad (2007) embarked on the controller design for minimizing size, enhancing efficiency and reliability of power converters in portable electronic equipment such as mobile phones and personal digital assistants (PDA).That was achieved with the use of a 90nm process with an input voltage of 1.55V and an output of 1V with a power dissipation of approximately 200mW.

Salvatore *et al* (2003) explained the use of supercaps as auxiliary devices of on board energy sources. It showed that they could successfully support current peaks, temporarily requested by electrical road vehicles. The co-action was useful to improve efficiency of the whole driving system and to take longer battery life. These advantages could be really reached in practice only by implementing proper control techniques. The paper suggested one of these techniques and by means of a digital simulation and some experimental tests gave evidence to many practical problems and to some possible solutions of them.

2.2 POWER SUPPLY FAMILY

Power supply is an essential component of a battery charger. Power supply can be categorised as linear power supply and switch mode power supply. The main difference is efficiency.

2.2.1 LINEAR POWER SUPPLY

Linear power supply provides significant advantages over switching regulators in simplicity, cost and output noise. The main disadvantage is the transformer operating at low frequency which is heavy, large, and expensive. It requires a large heat sink to dissipate heat generated by the regulating element and the efficiency is low.

2.2.2 SMPS POWER SUPPLY

Today the switch mode power supply (SMPS) with its high efficiency (70 – 80%), small size is already replacing the linear regulator in many applications where high efficiency and small size are of importance. Switch mode power supply shown in Figure 2.3 offers the possibility of theoretically lossless power conversion. It employs duty cycle control

of a switching element to block the flow of energy and thus achieve regulation. The switch mode power supply has the following additional advantages:

a) High switching frequency enables the use of a small ferrite transformer core.

b) It may operate in a much larger DC input voltage range (than the linear regulators)

c) It often has a higher efficiency.

Although the benefits of switch mode techniques are significant, there are some drawbacks.

Both the input and output present increased noise of the supply due to the power switching techniques, and the associated control circuitry is more complicated compared to the linear counterpart, e.g. an isolated feedback signal is needed for the control.

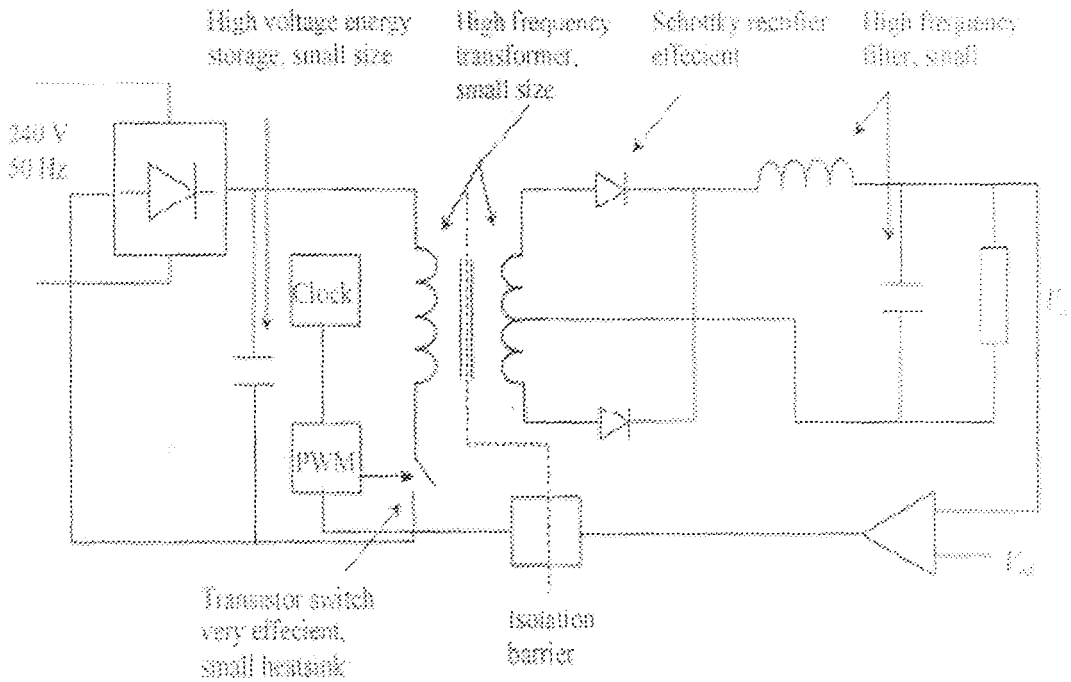

Figure 2.2: Block diagram of a SMPS (Mohammad)

2.3 TYPE OF BATTERY CHARGERS

Battery chargers can be divided into four basic design types:

- Linear Chargers
- Switch Mode Chargers
- Ferro resonant Chargers
- SCR Chargers

2.3.1 LINEAR CHARGERS

Linear chargers consist of a power supply, which converts AC power to lower voltage DC power, and a linear regulating element, which limits the current that flows into the battery. The power supply typically consists of a transformer that step down AC power from 220VAC to a lower AC voltage closer to that of the battery, and a rectifier that smooths out the existing sinusoidal AC signal into a constant-voltage DC signal. The linear regulating element may be a passive component such as a resistor or an active component such as a transistor that is controlled by a reference signal. Figure 2.3 shows a simplified schematic of a linear charger with a linear power supply with a resistor as the current regulating element.

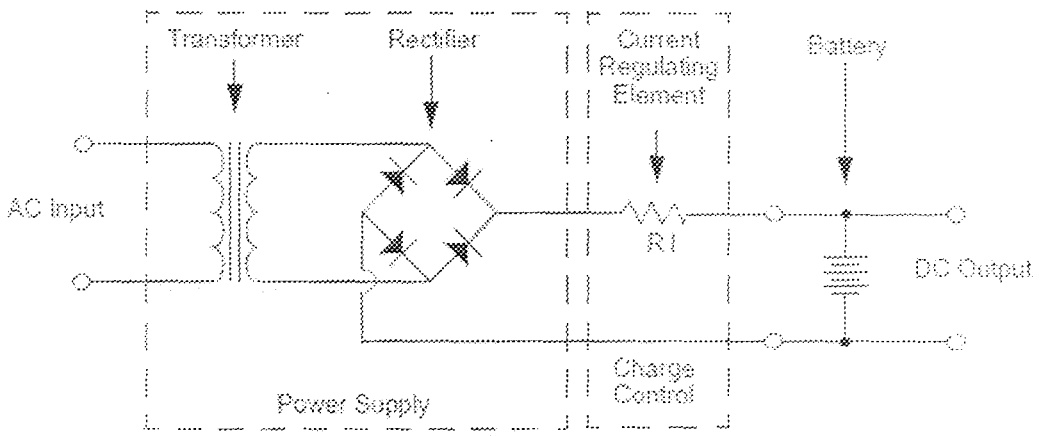

Figure2.3: A simplified schematic of a linear charger (Sagar *et al*).

2.3.2 SWITCH MODE CHARGERS

A switch mode charger rectifies AC voltage and then converts it to a lower DC voltage through a DC/DC converter. This type of charger contains additional charge control circuitry to regulate current flow into the battery. The charge control regulates the way in which the power switch turns ON and OFF, and may be accomplished through a circuit, a specialized integrated chip, or some type of software control. A simplified schematic for a single piece switch mode charger is shown in Figure 2.4.

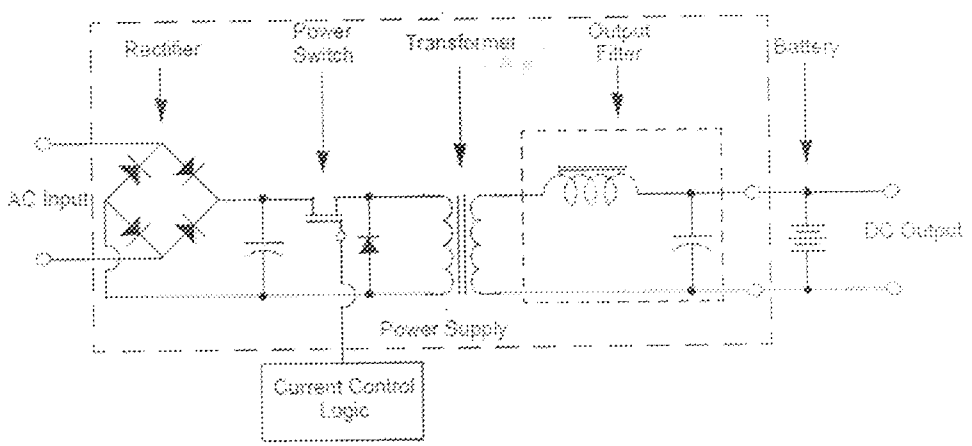

Figure2.4: Schematic for a single piece switch mode charger (Sagar *et al*).

2.3.3 SCR CHARGERS

SCR chargers use a special component known as a Silicon-Controlled Rectifier (SCR) to control the current to the battery. The SCR is a semi-controllable switch that can be turned ON and OFF (via commutation circuits) multiple times per second. After a transformer reduces utility voltage to a value near that of the battery, the diodes rectify the current while the SCR enables the flow of charge current according to a control signal. A block diagram of an SCR charger is shown in Figure 2.5

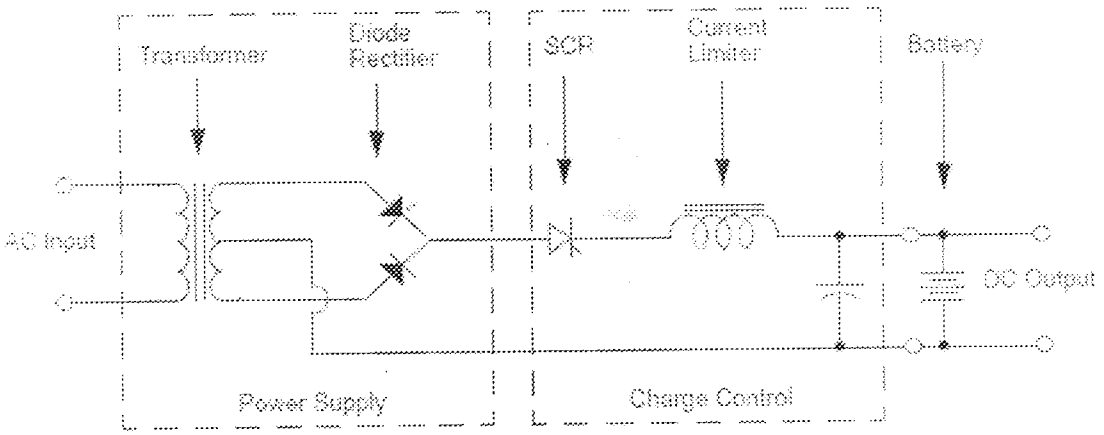

Figure: 2.5: A block diagram of an SCR charger (Sagar *et al*).

2.3.4 FERRORESONANT CHARGERS

Ferroresonant chargers (sometimes called ferro chargers), operate by way of a special component called a ferroresonant transformer. The ferroresonant transformer reduces the AC voltage to a lower regulated voltage level while simultaneously controlling the charge current. A rectifier then converts the AC power to DC power suitable for the battery. Figure 17 shows a block diagram of a ferroresonant charger.

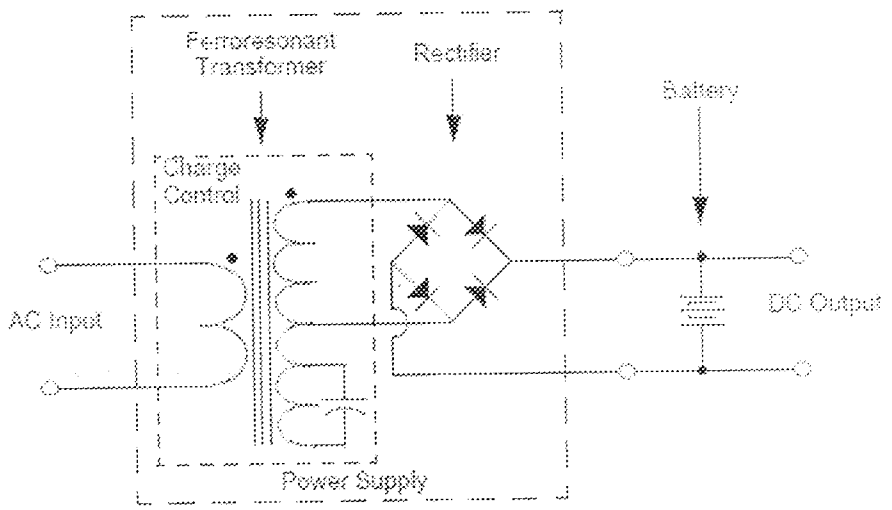

Figure 2.6: A block diagram of a ferroresonant charger (Sagar *et al*).

2.4 LEAD ACID BATTERIES

Lead Acid Batteries were invented in 1859 by Gaston Plante and first demonstrated to the French Academy of Sciences in 1860. They remain the technology of choice for automotive SLI (Starting, Lighting and Ignition) applications because they are robust, tolerant to abuse, tried and tested and because of their low cost. For higher power applications with intermittent loads however, Lead acid batteries are generally too big and heavy and they suffer from a shorter-cycle life and typical usable power down to only 50% Depth of Discharge (DOD). Despite these shortcomings Lead acid batteries are still being specified for PowerNet applications (36 Volts 2 kWh capacity) because of the cost, but this is probably the limit of their applicability. NiMH and Li-Ion baueries are making inroads into this market. For higher voltages and cyclic loads other technologies are being explored. Lead-acid batteries are composed of a Lead-dioxide cathode, a sponge metallic Lead anode and a Sulphuric acid solution electrolyte. This heavy metal element makes them toxic and improper disposal can be hazardous to the environment. The cell voltage is 2 volts.

Advantages

a) Inexpensive and simple to manufacture.

b) Mature, reliable and well-understood technology - when used correctly, lead-acid is durable and provides dependable service.

c) The self-discharge is among the lowest of rechargeable battery systems.

d) Low maintenance requirements - no memory; no electrolyte to fill on sealed version.

Limitations

a) Low energy density - poor weight-to-energy ratio limits use to stationary and wheeled applications. The cell voltage should never drop below 1.8V.

b) Allows only a limited number of full discharge cycles - well suited for standby applications that require only occasional deep discharges.

c) Lead content and electrolyte make the battery environmentally unfriendly.

d) Capable of high discharge rates.

Figure 2.3 shows the elements of a standard Lead – Acid battery.

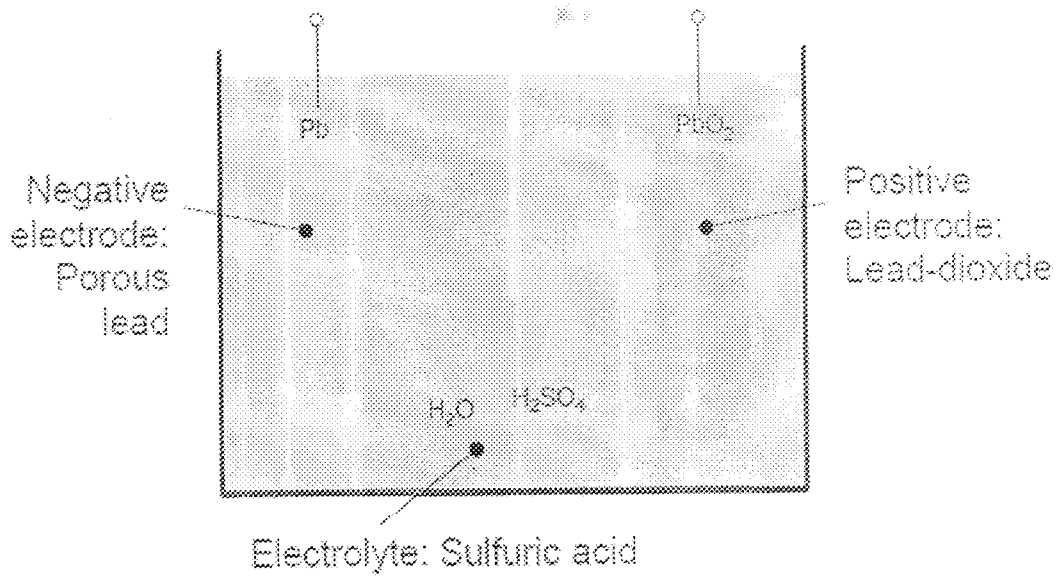

Figure 2.7: A diagram of a Lead Acid Battery (ECEN 4517/5517)

2.4.1 DISCHARGE

During discharge, the lead dioxide (positive plate) and lead (negative plate) react with the electrolyte of sulphuric acid to create lead sulphate, water and energy.

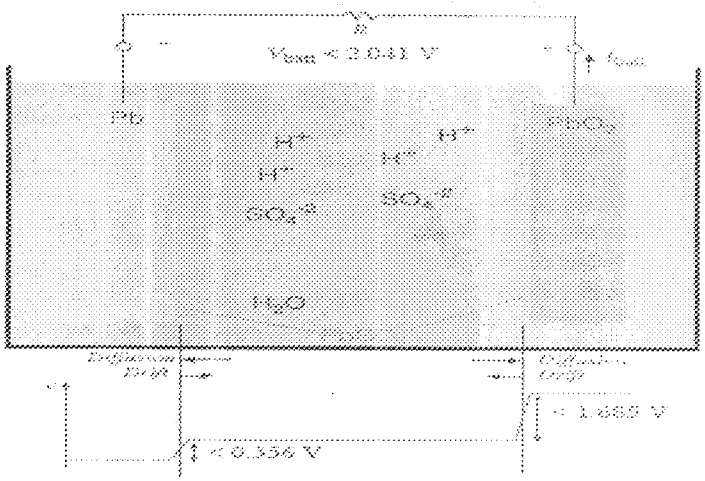

Figure 2.8: A block diagram of a positive and negative plate of a Lead – Acid battery (ECEN 4517/5517)

2.4.2 C - RATE

The charge and discharge current of a battery is measured in C-rate. The quantity C is defined as the current that discharges the battery in 1 hour, so that the battery capacity can be said to be *C* Ampere-hours. If the battery discharges more slowly, say at a current of *C*/10, then the battery would run longer (10 hours) before becoming discharged. In practice, the relationship between battery capacity and discharge current is not linear, and less energy is recovered at faster discharge rates. **Peukert's Law** relates battery capacity to discharge rate:

$Cp = I^k t$

Where Cp is the amp-hour capacity at a 1 A discharge rate

I is the discharge current in Amperes

t is the discharge time, in hours

k is the Peukert's coefficient, typically 1.1 to 1.3

2.4.3 BATTERY EFFICIENCY

Lead acid batteries typically have Coulombic efficiencies that vary from 70% to 84% (Science and engineering encyclopedia). It is the ratio (expressed as a percentage) between the energy removed from a battery during discharge compared with the energy used during charging to restore the original capacity. Also called charge efficiency or charge acceptance.

2.4.4 CHARGING

During charging, the cycle is reversed, the lead sulphate and water are electro-chemically converted to lead, lead oxide and sulphuric acid by an external electrical charging source. The objective of fast charging a battery is to cram as much energy as it takes to bring the battery back to fully charged state in the shortest possible time without damaging the battery or permanently affecting its long term performance. Since current is proportional to energy divided by time, the charging current should be as high as the battery systems will reasonably allow. The constant-potential cells (Lead-Acid and Lithium-Ion) are a bit slower to reach the 90 percent mark, but can generally be completely recharged within five hours, EG&G (2004). Fast-charging has compelling benefits, but places certain demands upon the battery system. A properly performed fast-charge, coordinated to the specifications of a battery rated for such charging, will deliver a long cycle life. The high charging rates involved, however, cause rapid electrochemical reactions within the cells of the battery. After the battery goes into overcharge, these reactions cause a sharp increase in internal cell pressure and temperature.

Uncontrolled high-rate overcharge quickly causes irreversible battery damage. Thus, as the battery approaches full charge, the charging current must be reduced to a lower "top-off" level, or curtailed entirely. (See Figures 2.5 and 2.6 show charge stages of a lead-acid battery)

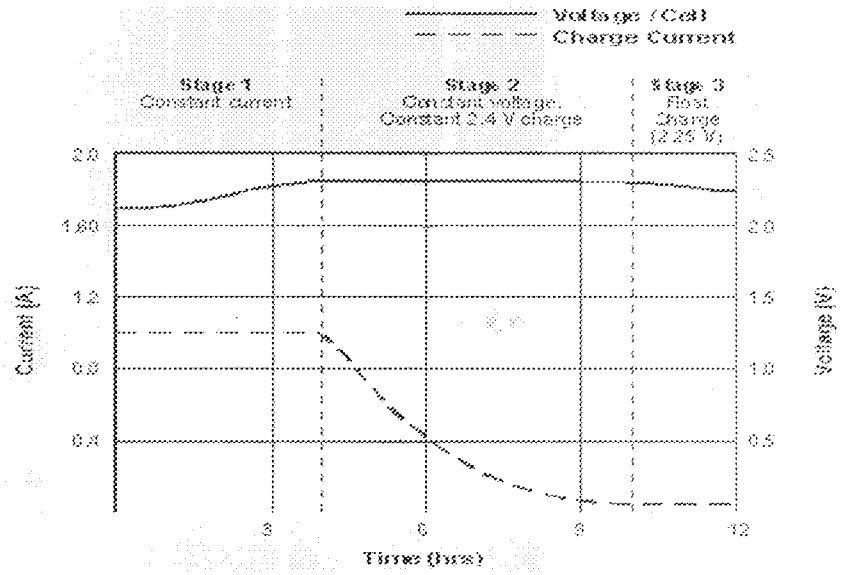

Figure 2.9: Showing charge stages of a lead-acid battery.

The battery charges at a constant current to a set voltage threshold (Stage 1). As the battery saturates, the current drops (Stage 2). The float charge compensates for the self-discharge (Stage 3) (http:Wikipedia)

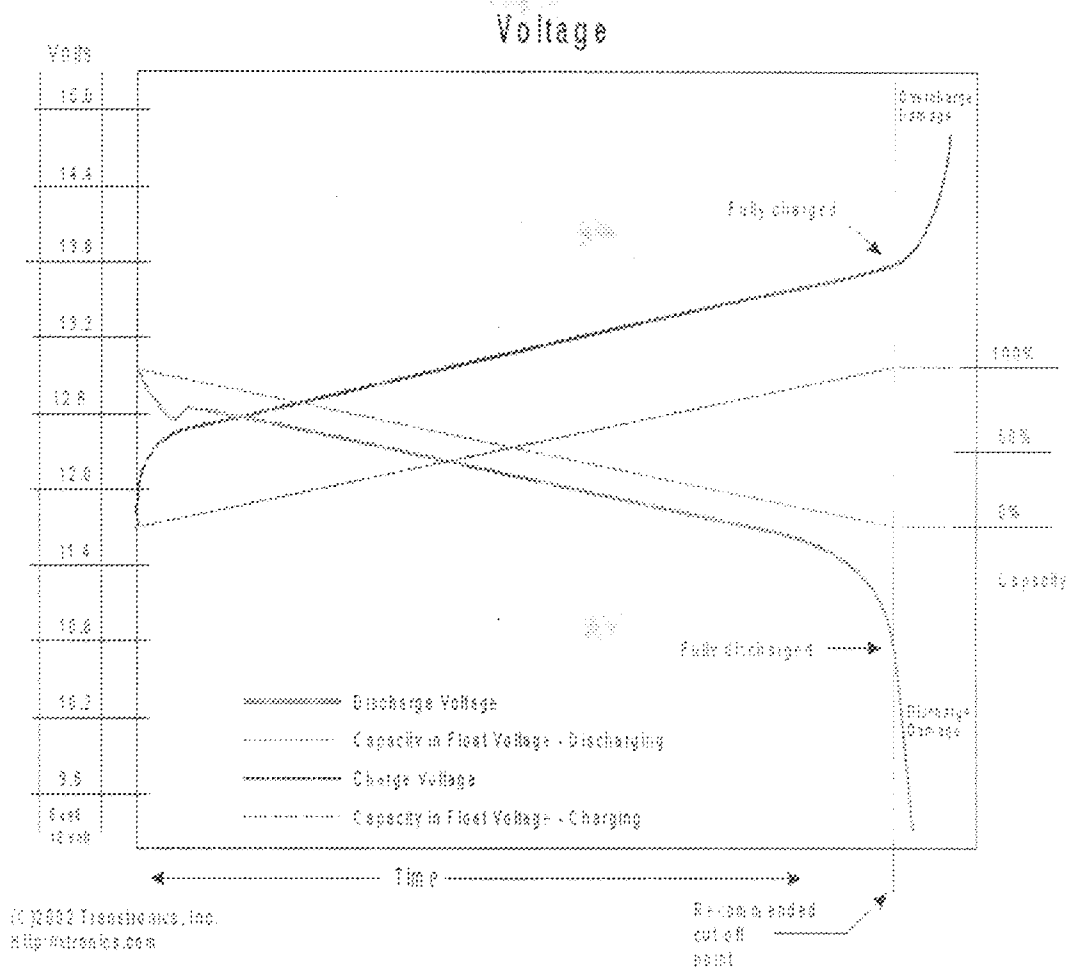

Figure 2.10: Showing the graph of 12V battery versus capacity at various stages of charge and discharge capacity (Http:Wikipedia)

CHAPTER THREE

3.0 MATERIALS AND METHOD

3.1 INTRODUCTION

This chapter presents the required materials, design procedure and the method adopted for the implementation of the SMPS battery charger.

3.1.1 SPECIFICATIONS

The objective of this project is to develop a half bridge push pull battery charger with 210 Watt output with the following specifications:

1) Minimum efficiency of 70%
2) Output voltage of 42V
3) Use of MOSFET IRF460 as switching devices
4) Line Input: 220 volts -15%, +10% (187 - 242 volts), 50Hz.
5) Main Output:

Voltage	: 42 volts
Current	: 5Amp
Current limit	: 10Amp
Over-voltage limit	: +10% of output voltage (46.2V)
Under-voltage limit	: -10% of output voltage (37.8V)
Ripple voltage	: less than 50 mVp-p maximum

6) Switching frequency : 100kHz

7) **Determination of the total period T**

With a switching frequency, f = 100kHz

$$T = \frac{1}{f} \tag{3.1}$$

$$T = \frac{1}{100{,}000} = 10\mu s$$

8) **Determination of the secondary Output Power, (P_o)**

$$P_o = I_o(V_o + V_d) \tag{3.2}$$

where I_o = output current,

V_o = output voltage and

V_d = Diode voltage = 1

$P_o = 5(42 + 1)$

$P_o = 215W$

9) **Determination of total Input Power (P_{in})**

$$P_{in} = \frac{P_o}{efficiency} = \frac{P_o}{\eta} = \frac{215}{0.7} = 307.14W \tag{3.3}$$

With minimum efficiency of 70%

10) **Determination of apparent power, (S)**

With power factor of 0.8 is assumed, we have apparent power as

$S = 307.14/0.8 = 384VA$ (3.3a)

3.2 THE BLOCK DIAGRAM ANALYSIS

Block diagrams of the 210 Watt 100 kHz SMPS is shown in Figure.3.1 and 3.2.

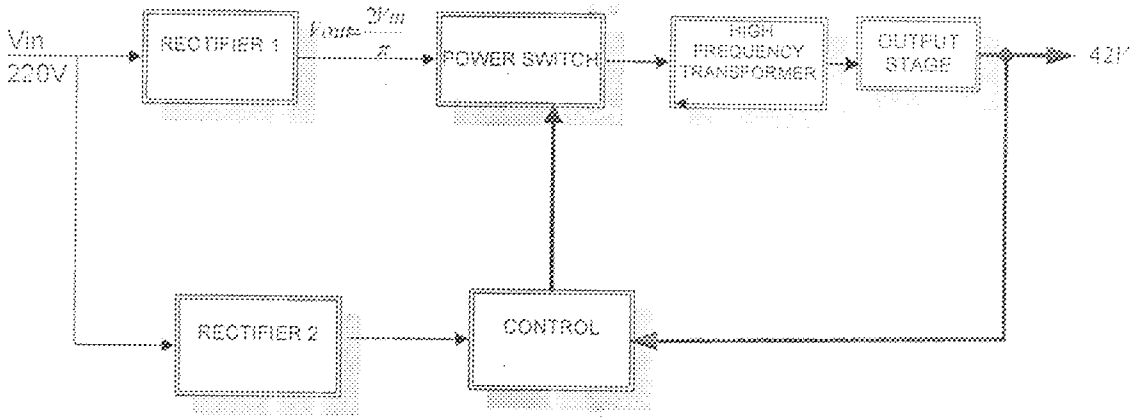

Figure 3.1: A block diagram of a SMPS

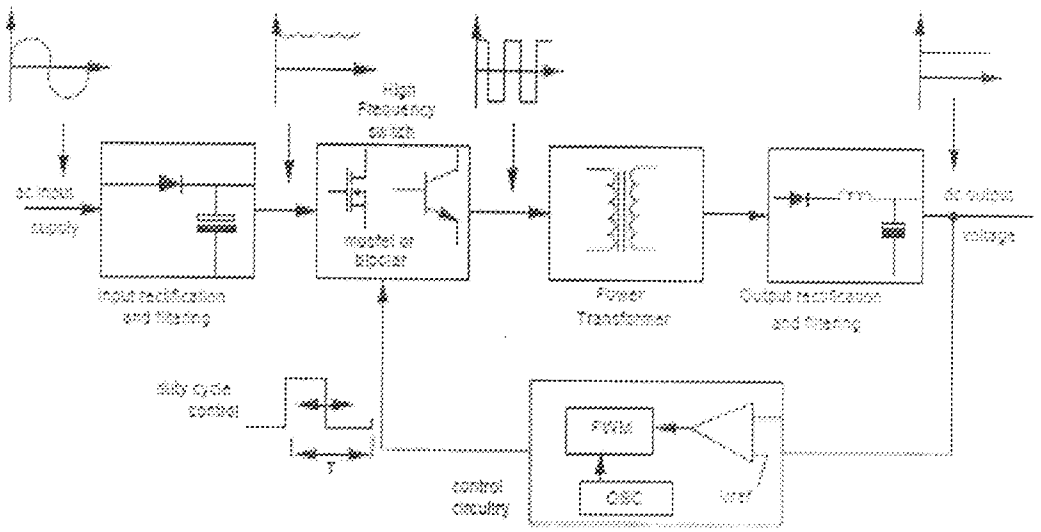

Figure 3.2: A block diagram with various stages of a SMPS (Phillip semiconductor)

3.2.1 INPUT RECTIFIER 1

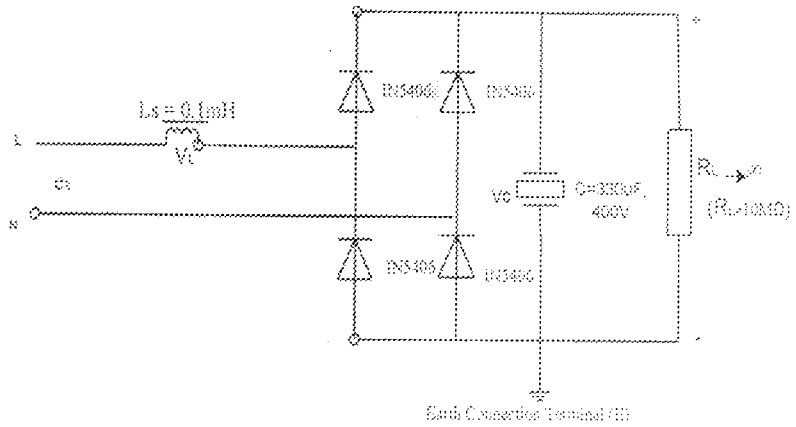

Figure 3.3: Showing main input rectifier 1

The rectification is achieved by using a bridge rectifier consisting of four diodes as shown in fig.3.3. Rectification is conversion of an AC input with zero DC average to a nonzero DC output along with some ripples.

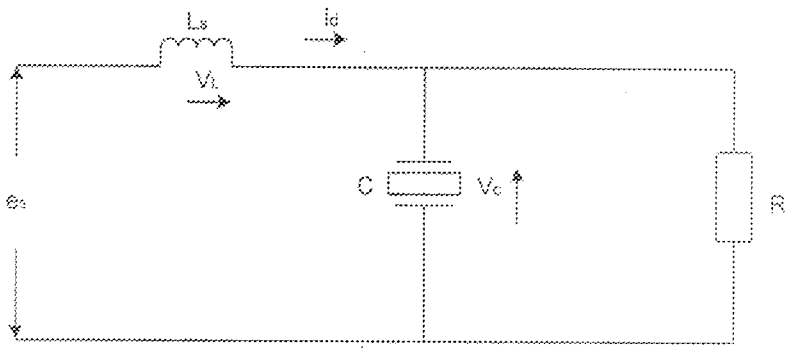

Figure 3.4: Showing equivalent circuit of input rectifier 1

By appling Kirchoff voltage law (KVL), in Figure 3.4, we have.

$V_L = L\frac{di}{dt}$ voltage across inductor L (3.4)

$$e_s = V_{L_s} + V_c \tag{3.5}$$

$$e_s = \frac{L_s di_s}{dt} + Vc \tag{3.6}$$

$$\frac{di_s}{dt} = -\frac{1}{L} V_c + \frac{1}{L} e_s \tag{3.7}$$

By also applying Kirchhoff's current law (KCL) in circuit shown in figure 3.4

$$\frac{dV_c}{dt} = -\frac{1}{CR_L} V_c + \frac{1}{C} i_s \tag{3.8}$$

By applying state space equation to equation 3.7 and 3.8, we have

$$X(t) = AX(t) + BU(t) \tag{3.9}$$

$$\begin{bmatrix} \frac{dV_c}{dt} \\ \frac{di_s}{dt} \end{bmatrix} = \begin{bmatrix} -\frac{1}{CR_L} & \frac{1}{C} \\ -\frac{1}{L_s} & 0 \end{bmatrix} \begin{bmatrix} V_c \\ i_s \end{bmatrix} + \begin{bmatrix} 0 \\ \frac{1}{L_s} \end{bmatrix} e_s \tag{3.10}$$

C=330μF, R_L=10MΩ, L_S= 0.1mH.

$$\begin{bmatrix} \frac{dVc}{dt} \\ \frac{di_s}{dt} \end{bmatrix} = \begin{bmatrix} -\frac{1}{330\times10^{-6}\times10\times10^{6}} & \frac{1}{330\times10^{-6}} \\ \frac{1}{0.1\times10^{-3}} & 0 \end{bmatrix} \begin{bmatrix} V_c \\ i_s \end{bmatrix} + \begin{bmatrix} 0 \\ \frac{1}{0.1\times10^{-3}} \end{bmatrix} e_s \tag{3.11}$$

$$\begin{bmatrix} \frac{dVc}{dt} \\ \frac{di_s}{dt} \end{bmatrix} = \begin{bmatrix} -3.03\times10^{-4} & 30.3 \\ -10.000 & 0 \end{bmatrix} \begin{bmatrix} V_c \\ i_s \end{bmatrix} + \begin{bmatrix} 0 \\ 10.000 \end{bmatrix} e_s \tag{3.12}$$

The solution to equation 3.10 to 3.12c is obtained by trapezoidal rule of integration by using Matlab software. The Matlab code is attached in appendix 3.

$$x(t) = Mx(t-\Delta t) + N\left[\left|e_s(t)\right| - \left|e_s(t-\Delta t)\right|\right] \tag{3.12a}$$

$$M = \left[I - \frac{\Delta t}{2}A\right]^{-1}\left[I + \frac{\Delta t}{2}A\right] \tag{3.12b}$$

$$N = \left[I - \frac{\Delta t}{2}A\right]^{-1}\frac{\Delta t}{2}B \tag{3.12c}$$

After much iteration, the final value obtained for the state space equation is given below with the corresponding voltage across capacitor shown in figure 3.4a while figure 3.4b shows the capacitor current and figure 3.4c shows the combination of the source voltage (e_s) with the capacitor voltage (V_c) and capacitor current (I_s) obtained.

$$x = \begin{bmatrix} V_c \\ I_s \end{bmatrix} = \begin{bmatrix} 190.00 \\ 0.0000 \end{bmatrix} \tag{3.12d}$$

Also the graph shown in Figure 3.4a was the rectifying voltage across the capacitor, while Figure 3.4b was the rectifying current across the capacitor and Figure 3.4c shows comparison of the capacitor voltage Vc, capacitor current Ic and supply voltage e_s plotted against time t.

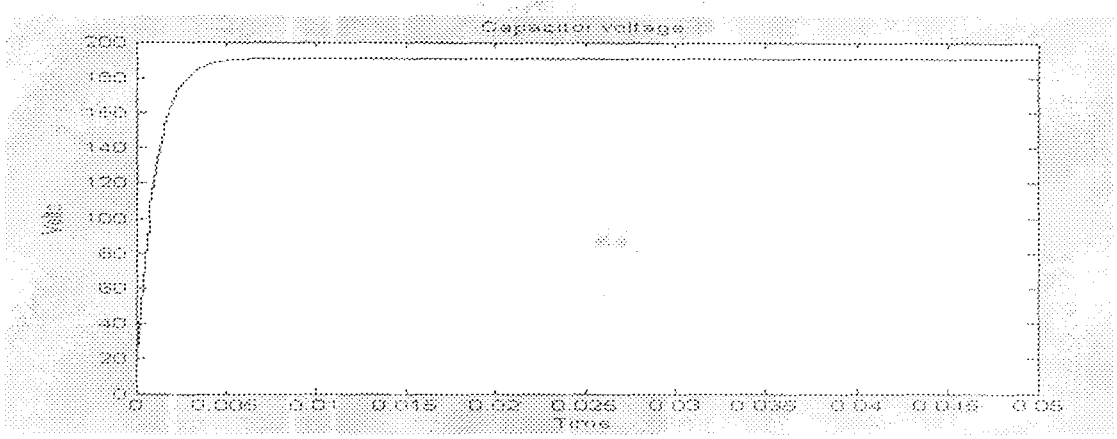

Figure 3.4a: Showing graph of Vc against time

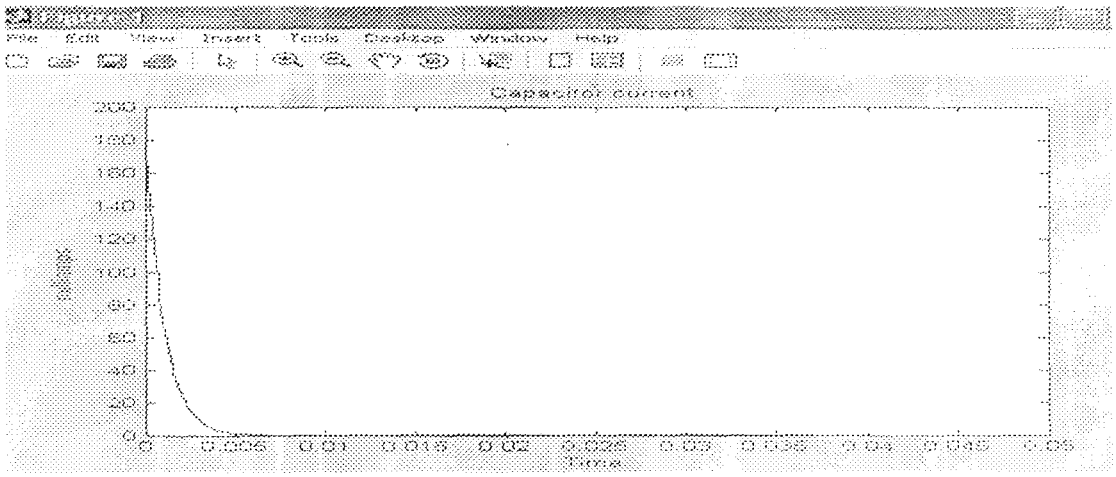

Figure 3.4b: Showing the graph of Ic against time

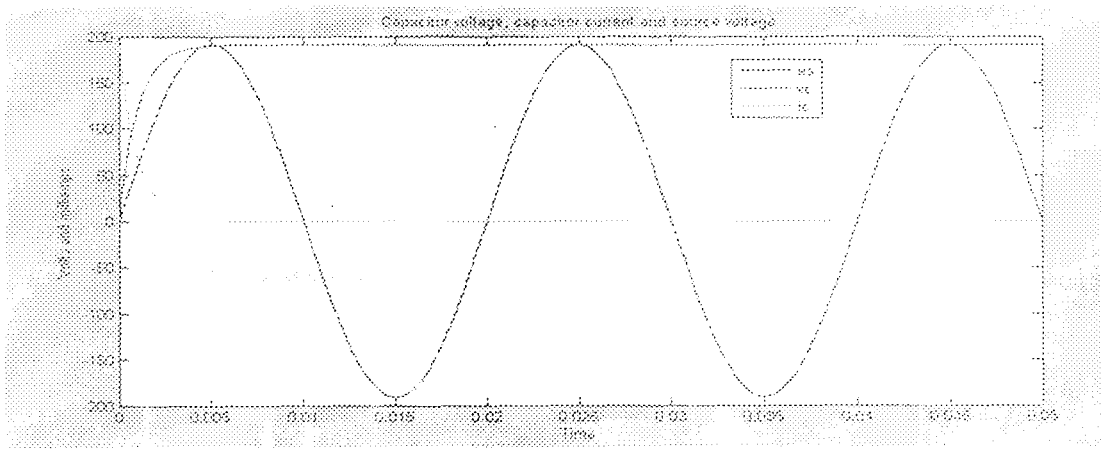

Figure 3.4c: Showing the graph of V_c, I_c, and e_s against time

3.2.2 FILTERING CAPACITOR

To reduce the AC ripple riding on the DC output, a capacitor of 330μF, 400V is used for filtering. The filtering effect of the capacitor can be understood as shown in figure 3.4

The voltage V_{dc} is the average output dc voltage

$$V_{dc} = 2Vm/\pi \qquad (3.13)$$

Where V_m = Peak value of input A/C

$V_m = 220\sqrt{2}$

$V_m = 311V$

$$V_{dc} = 2 \times 311/\pi = 198V \qquad (3.14)$$

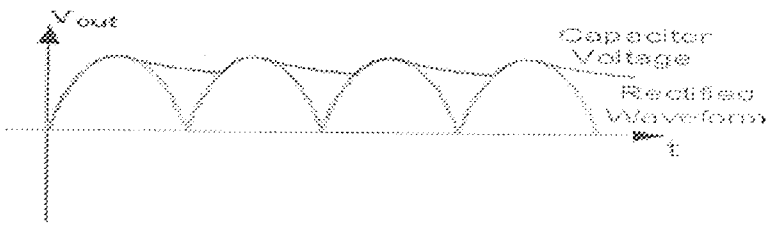

Figure 3.5: A block diagram of a Filter Output

3.2.3 INPUT RECTIFIER 2

The auxiliary power supply shown in figure 3.5 provides power to the control IC SG3524 through the bridge rectifier and the LM7809 regulator which drives the circuits of the converter from the initial start-up stage to the continuous operating mode of the converter.

3.2.4 THE POWER SWITCHES MOSFET (IRF450)

This section converts dc-ac and regulates the ac output voltage. The Mosfet IRF450 is called high frequency switch. It controls the duty cycle $d(t)$. T_1 and T_2 switches shown in figure 3.6 are alternately turned-on during a time t_{on}. The power switches or MOSFETS as used in the design, switch very fast between saturation and cut-off. The MOSFETS act as "gates", which control the amount of energy to be transferred from the input to the load. The amount of energy to be transferred is determined by the control circuit, which determines the "on" time for the MOSFETS, depending on the demand of the load.

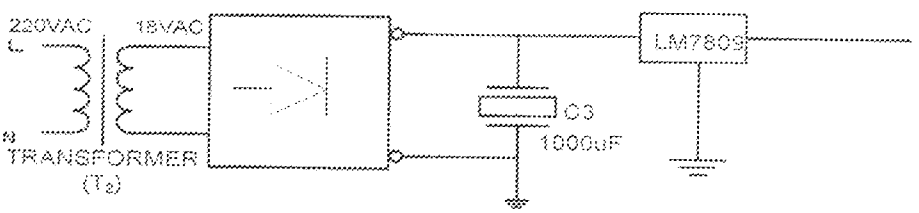

Figure 3.6: Showing auxiliary rectifier 2

The secondary circuit operates at twice the switching frequency. A dead time t_d between the end of conduction of one switch and the turn-on time of the other one is required in order to avoid simultaneous conduction of the two switches.

The power MOSFET IRF450 has three terminals: drain, gate, and source. The gate to source voltage controls the conduction state of the power MOSFET. There is an insulating layer between the gate and an electrostatically controlled conduction channel between the drain and the source. Application of a gate to source voltage greater than the device threshold voltage will cause the power MOSFET to turn on by modulating the geometry of the electrostatic conduction channel

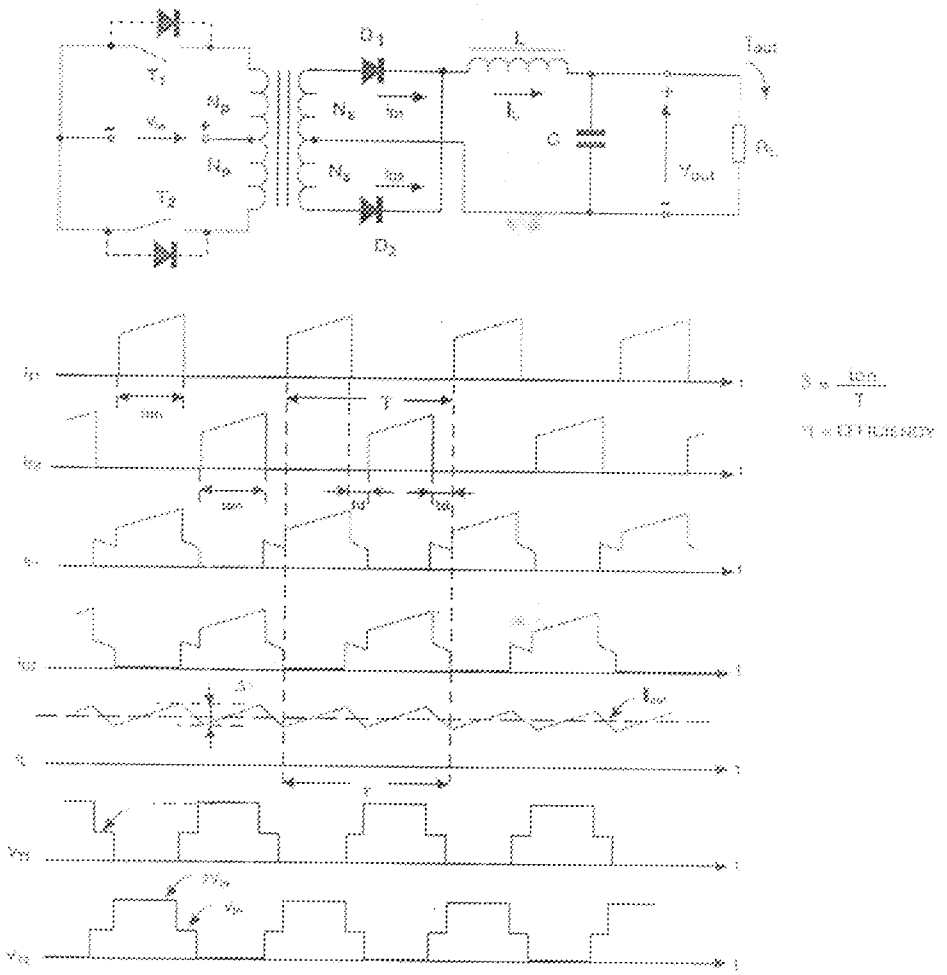

Figure 3.7: Showing switching operation of T_1 and T_2

3.2.5 CONTROL SECTION

It comprises the oscillating, comparator and the PWM stage. Figure 3.7 shows the control circuit as it is configured for this design. The integrated circuit used is the SG3524 which is a pulse width modulated (PWM) control circuit. The double totem-pole output drive circuit of the SG3524 can sink and source up to 200 mA. The complementary output allows either single-ended or push-pull application. Each device includes an on-chip regulator, error amplifier, programmable oscillator, pulse-steering flip-flop, two uncommitted pass transistors, a high-gain comparator, and current-limiting and shutdown circuitry. The SG3524 contains an onboard 5V regulator that

serves as a reference, as well as supplying the SG3524 internal regulator control circuitry. The oscillator output serves as blanking pulse to ensure both outputs are never on simultaneously during the transition times.

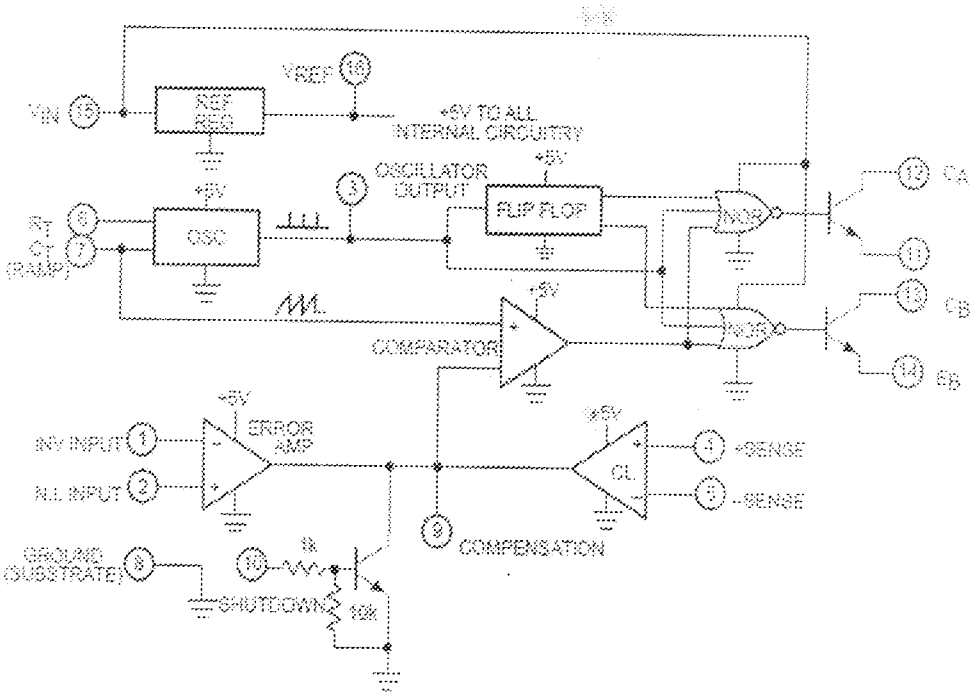

Figure 3.8: A schematic diagram of control IC- SG3524 (Phillips semiconductor)

3.2.6 OSCILLATOR

The oscillator controls the frequency of the SG3524 and is programmed by R_T and C_T according to the approximate formula:

$$f = \frac{1.18}{R_T C_T} \qquad (3.15)$$

where: R_T is in KΩ, C_T is in μF and f is in KHz

Practical values of C_T fall between 0.001 and 0.1μF. Practical values of R_T fall between 1.8 and 100KΩ. This results in a frequency of 590 KHz, when R_T = 2 kΩ and C_T = 0.001μF.

3.2.7 COMPARATOR AND PWM

A differential amplifier is used to sense the difference between an ideal voltage (the reference voltage of 2.5V) and the actual output voltage to establish a small error signal. Figures 3.8a and 3.8b show the block diagrams. The heart of a switching power supply is its switch control circuit (controller). Often, the control circuit is a negative-feedback control loop connected to the switch through a comparator and a Pulse Width Modulator (PWM). The switch control signal (PWM), controls the state (ON or OFF) of the switches. This control circuit regulates the output voltage against changes in the load and the input voltage.

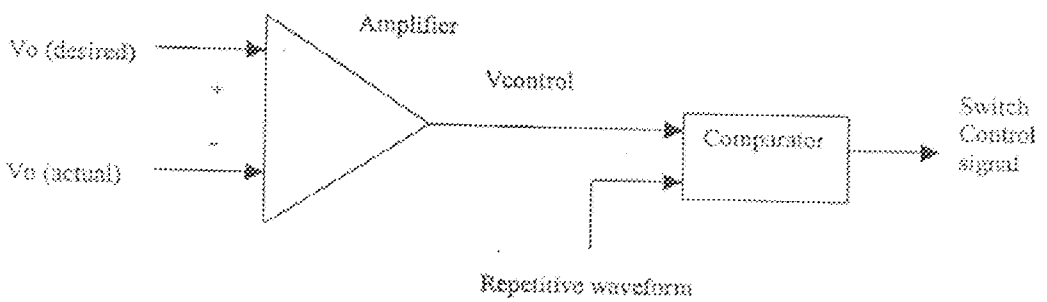

Figure 3.9a: Comparator Signals for PWM

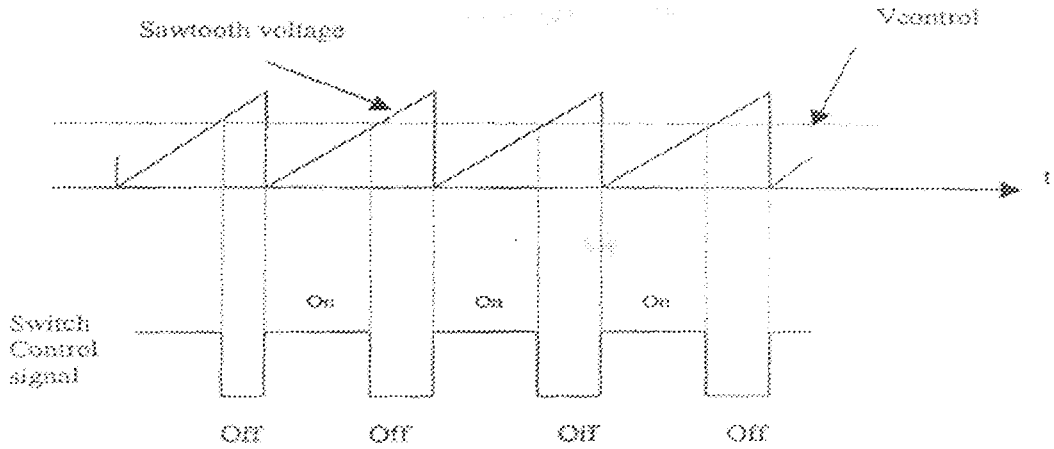

Figure 3.9b: Comparator Signals showing T_{on} and T_{off}

3.2.8 TRANSFORMER SECTION

The push-pull configuration is normally used for output powers in the 100 to 500W range. This Section covers the design of power transformers used in buck-derived push pull half-bridge topology. The power transformer provides the required isolation between the input and the output. In this configuration the transformer stores no energy, but is simply used to step down the high frequency input voltage and generate the output voltage as required for this design. .

Power is transferred to the output circuit during each transistor conduction period. The duty ratio of each switch is usually less than 0.45. This provides enough dead time to avoid transistor cross conduction. The power is transferred to the output for up to 90% of the switching period.

3.2.9.3 Determination of the secondary rms current, Is(rms).

$$Isrms = Is\sqrt{D\max} \tag{3.29}$$

Dmax = maimum duty ratio = 0.5 and I_s = secondary current = 5A

$$= 5 \times \sqrt{0.5} = 5$$

$$= 5 \times 0.7071 = 3.535A$$

3.2.9.4 Determination of the secondary base wire area, Aws.

$$Aws(B) = \frac{Isrms}{J} \tag{3.30}$$

And current density = 152.17A/cm^2

$$\frac{3.535}{152.17} = 0.0232cm^2 = 2.32\text{mm}^2$$

3.2.9.5 Determination of the required number of secondary strands, NSs

$$NSs = \frac{Aws(B)}{SWG19} = \frac{0.0232}{0.009} = 2.577 \quad \text{(3 strands was used)} \tag{3.31}$$

3.2.9.6 Determination of the secondary new mW per centimetre using 19SWG

$$(new)\mu\Omega/cm = \frac{\mu\Omega/cm}{NSs} = \frac{209.5}{3} = 69.83 \tag{3.32}$$

3.2.9.7 **Determination of winding resistance, Rs.**

$$Rs = MLT \times N_s \left(\frac{\mu\Omega}{cm}\right) \times 10^{-6} = 7.1 \times 3 \times 69.83 \times 10^{-6} = 0.001487\Omega \quad (3.33)$$

3.2.9.8 **Determination of secondary copper loss, Ps**

$$Ps = IsrmsRs$$

$$= (3.535)^2 \times 0.001487 = 0.01858W \quad (3.34)$$

3.2.9.9 **Determination of the total copper loss, Pcu**

$$Pcu = P_p + P_s = 0.06396 + 0.01858 = 0.0825W \quad (3.35)$$

3.3 OUTPUT RECTIFIERS

The output rectifier diodes are schoutky for this converter; the bipolar square waves at the secondary side of the power transformer are converted to unipolar square waves at twice the operating frequency. Half bridge is chosen for simplicity and to reduce cost as against the full bridge.

3.4 HEAT SINK

Heat sink is always considered to be of great importance in the designing of a half bridge converter. Due to fast switching of the MOSFET, a lot of heat is dissipated and this creates a very hot climate for the device to be operated in. Every device has a

maximum operating temperature. The N-channel MOSFET used in this converter also has a maximum operating temperature.

Total Power Dissipated at 25°C (Case) is 15W

From the above, we can determine the maximum temperature that the MOSFET can operate in,from the relationship below (Lian).

$$R_{\theta SA} = \frac{T_j - T_a}{P_d} - R_{\theta jc} - R_{\theta cs} \qquad (3.36)$$

T_j = maximum junction temperature in °C = $T_j = 90^{\circ}C$

T_a = maximum ambient temperature = $30^{\circ}C$

P_d = Power dissipated at 25°C = $15W$

$R_{\theta jc}$ = maximum allowable junction to case thermal resistance = $R_{\theta jc} = 1^{\circ}C/W$

$R_{\theta cs}$ = maximum allowable case to sink thermal resistance = $R_{\theta cs} = 0.5^{\circ}C/W$

$R_{\theta sa}$ = maximum heat sink to ambient thermal resistance

$$R_{\theta sa} = \frac{T_j - T_a}{P_d} - R_{\theta jc} - R_{\theta cs} \qquad (3.37)$$

$$R_{\theta sa} = \frac{90 - 30}{15} - 1 - 0.5 \qquad (3.38)$$

$$R_{\theta sa} = \frac{60}{15} - 1.5 \qquad (3.39)$$

$$R_{\theta sa} = 4 - 1.5 \qquad (3.40)$$

$$R_{sa} = 2.5^{\circ}C/W \qquad (3.41)$$

The R_{hsa} (Calculated) is 2.5°C/W

But from data sheet, heat sink selected must be smaller than calculated value.

Then heat sink number 6 was chosen from figure 3.11, which has a volume of 298(cm^3)

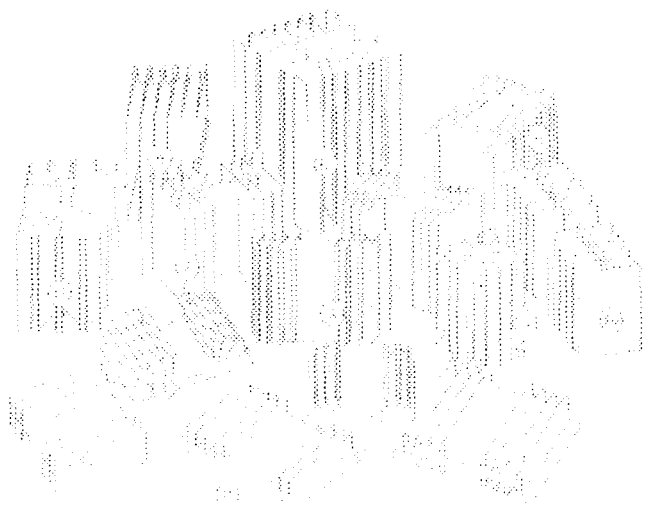

Heat sink no.	1	2	3	4	5	6	7	8	9	10	11	12
R_{hsa}(°C/W)	3.2	2.3	2.2	0	2.1	1.7	1.5	1.3	1.25	1.2	0.8	0.65
Vol. (cm^3)	76	99	181	0	198	298	435	675	608	634	695	1311

Figure 3.11: Heat sinks' data sheet (Lian Wan Heng)

3.5 Complete circuit of 42V SMPS battery charger

3.5 Complete circuit of 42V SMPS battery charger

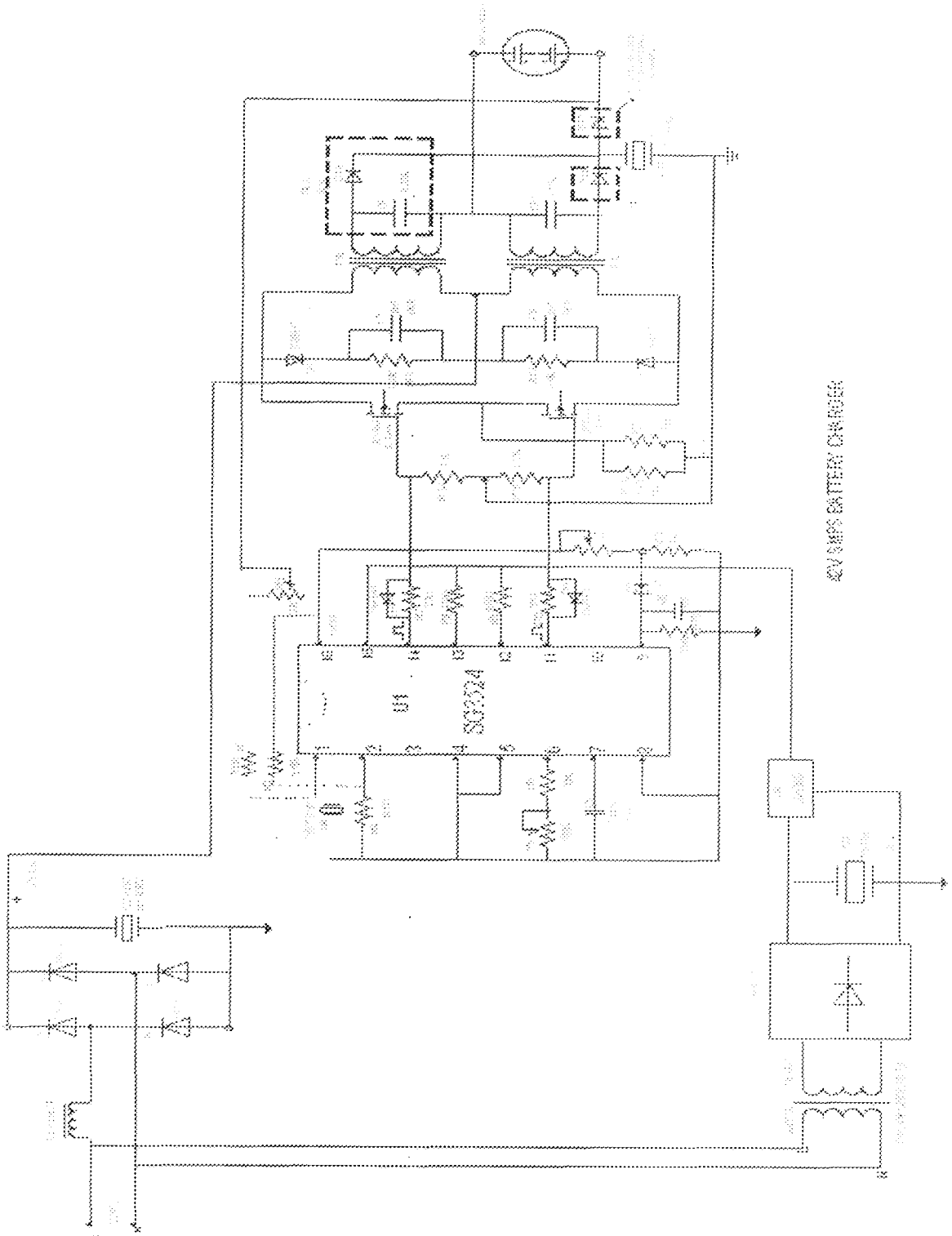

Figure 3.12: Complete circuit of 42V SMPS battery charger

3.4 Picture of the complete prototype is shown in plate I, while power switch IRF 450 is shown in plate II.

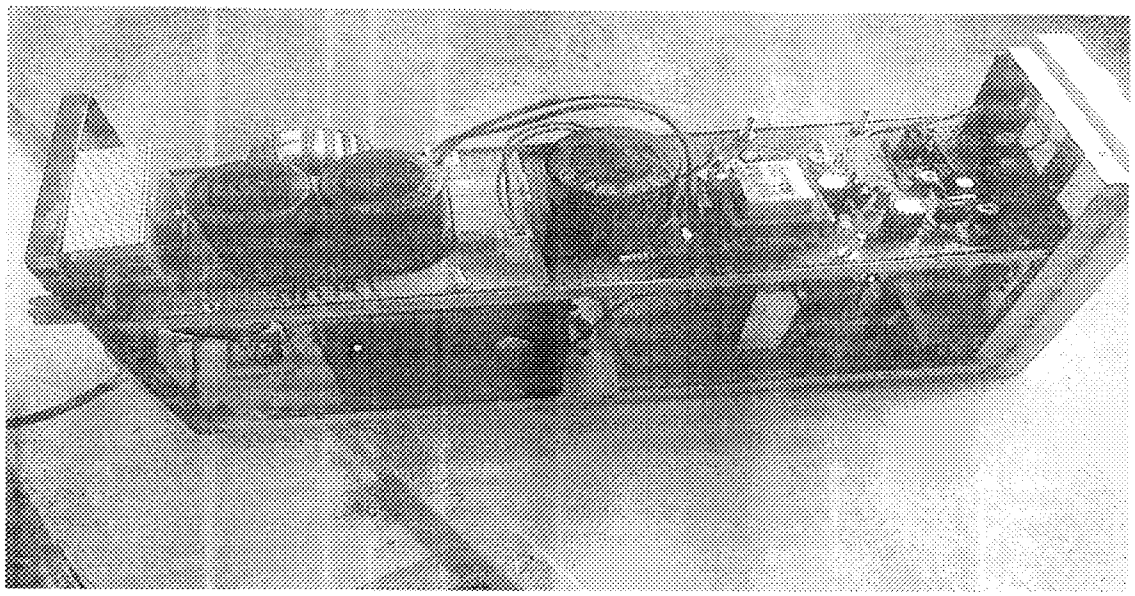

Plate I: Picture of the prototype

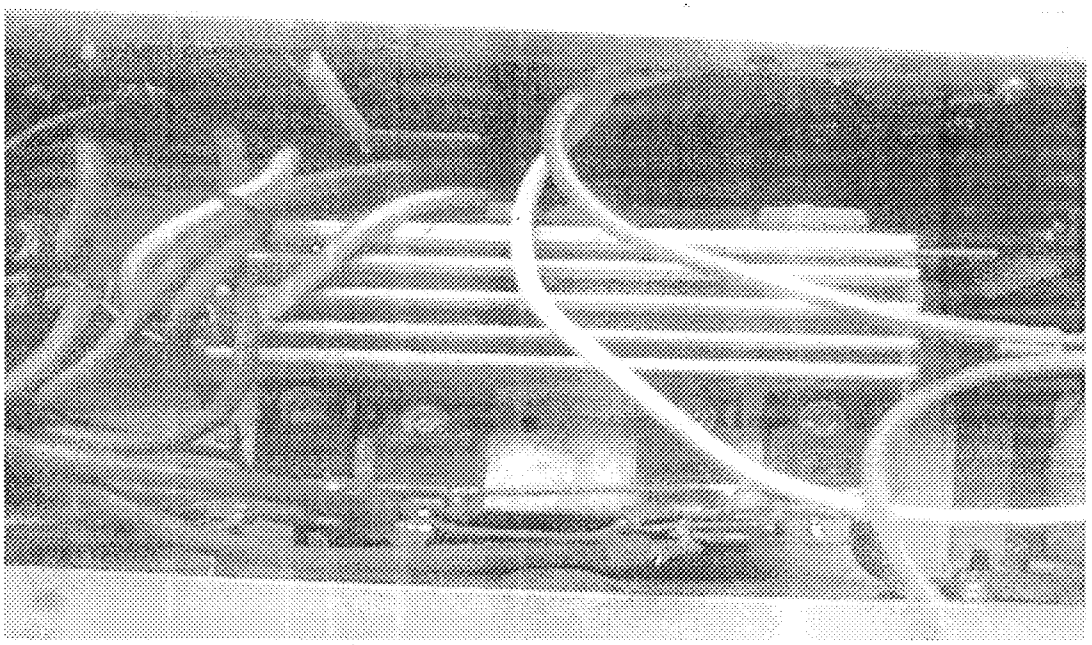

Plate II: Picture of the power switch IRF 450 mounted on heat sink

CHAPTER FOUR

4.0 RESULTS

4.1 INTRODUCTION

Using components listed in table 4.2, the battery charger was built. Details of results obtained from the experiment are presented, starting from the input rectifying stage, control stage and the output stage. Heat sink provided for the Mosfet.

4.2 CONSTRUCTION LAYOUT

The construction stages are shown in figures below:

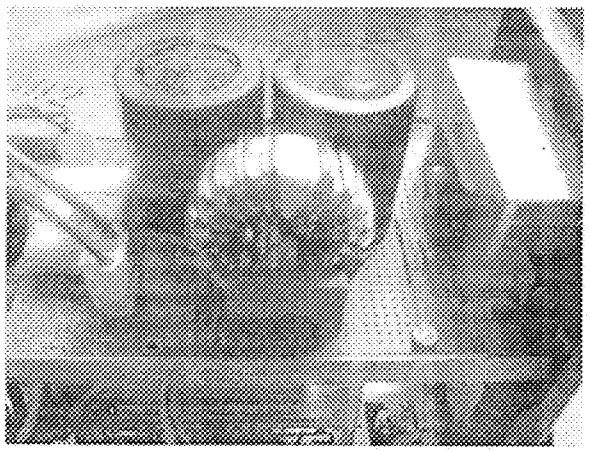

Plate III: Input supply protection stage.

Plate IV:Construction stage.

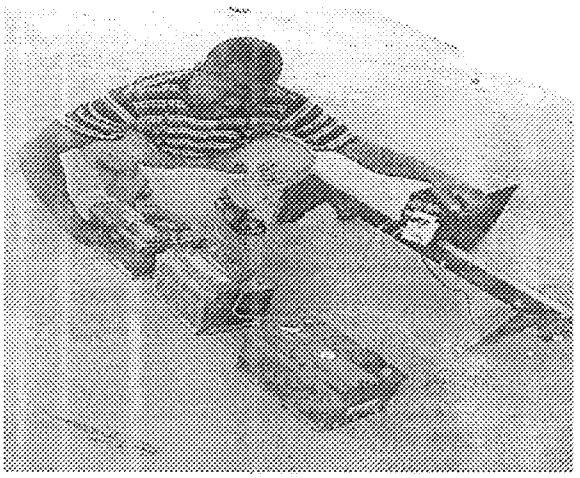

Plate V: Testing of 3 nos. of 12V battery in series

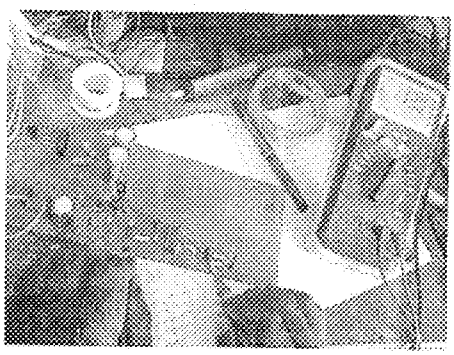

Plate VI: Testing Stage.

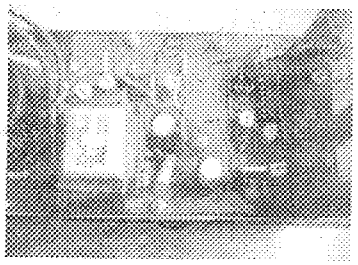

Plate VII: Testing Stage.

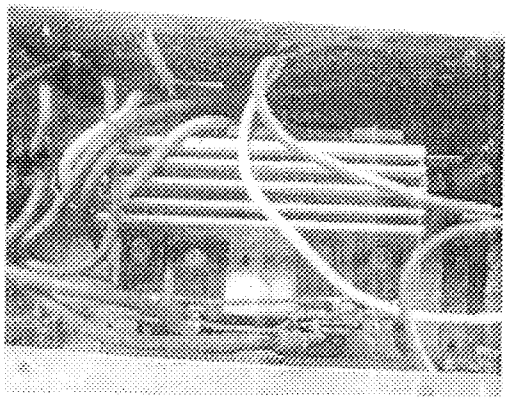

Plate VIII: Mosfet IRF 450 section

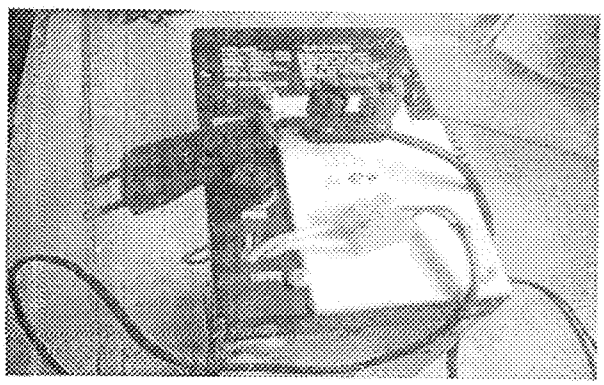

Plate IX: 36V Output terminal of the barger.

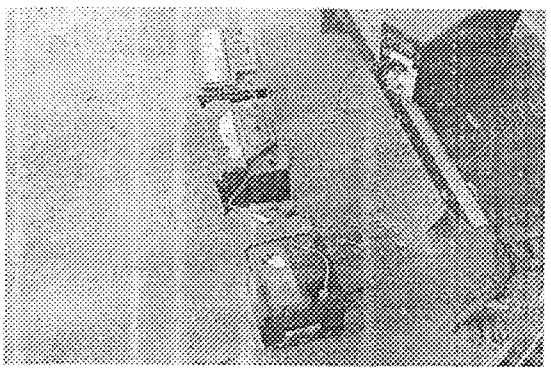

Plate X: Testing of 3 nos. of 12V connected in series to obtain 36V

4.3 RECTIFIER 1 WITHOUT FILTER CAPACITOR

Figure 4.3 shows the simulation result obtained showing ripple in the ouput dc line of rectifier 1 when the capacitor C_2 was not connected. The ripple signal was designated by blue colour, while the AC sinusoidal was designated with red colour.

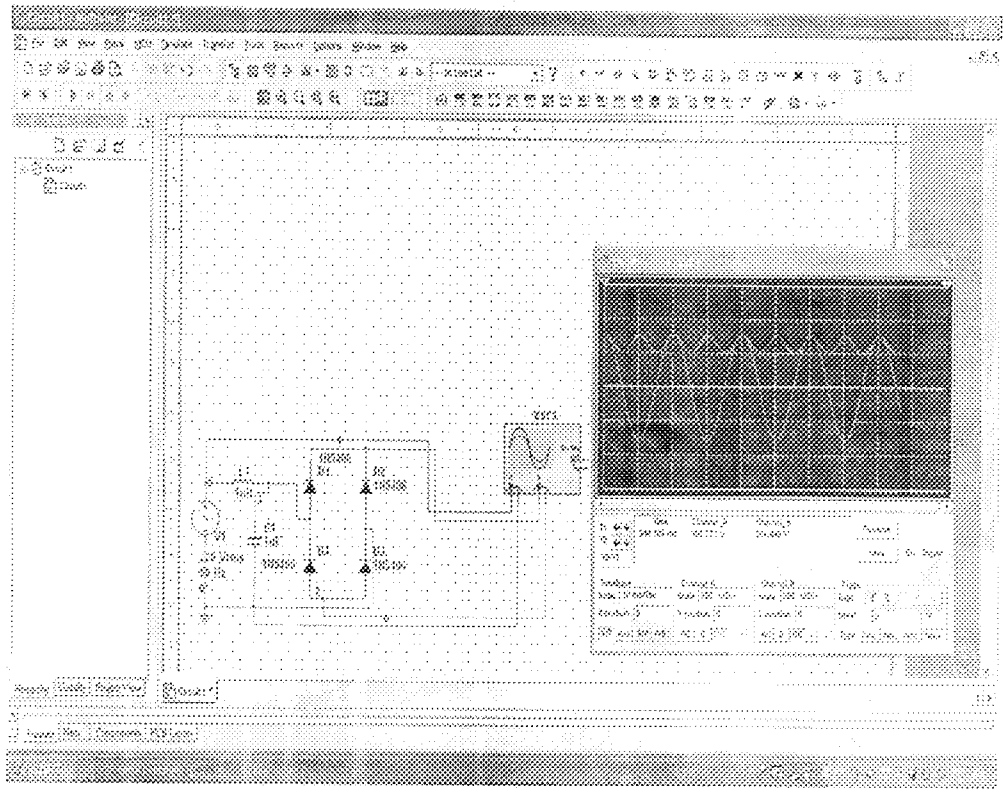

Figure 4.1: Rectifier 1 without filter capacitor

4.3.1 RECTIFIER 1 WITH FILTER CAPACITOR

Figure 4.4 shows the simulation result obtained without ripple in the ouput dc line of rectifier 1 when the capacitor C_2 was connected. The DC output signal was designated with blue colour, while the AC sinusoidal was designated with red colour.

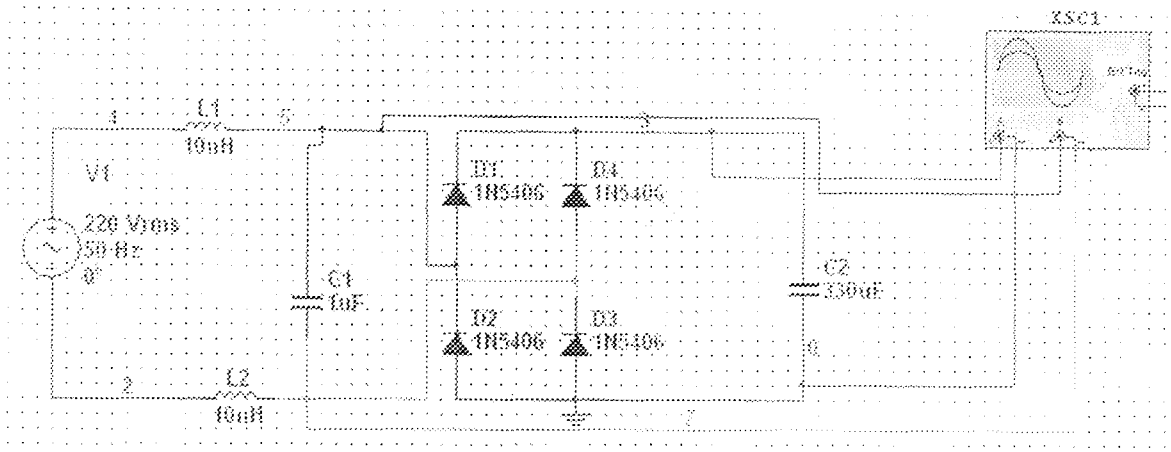

Figure 4.2: Rectifier 1 with filter capacitor.

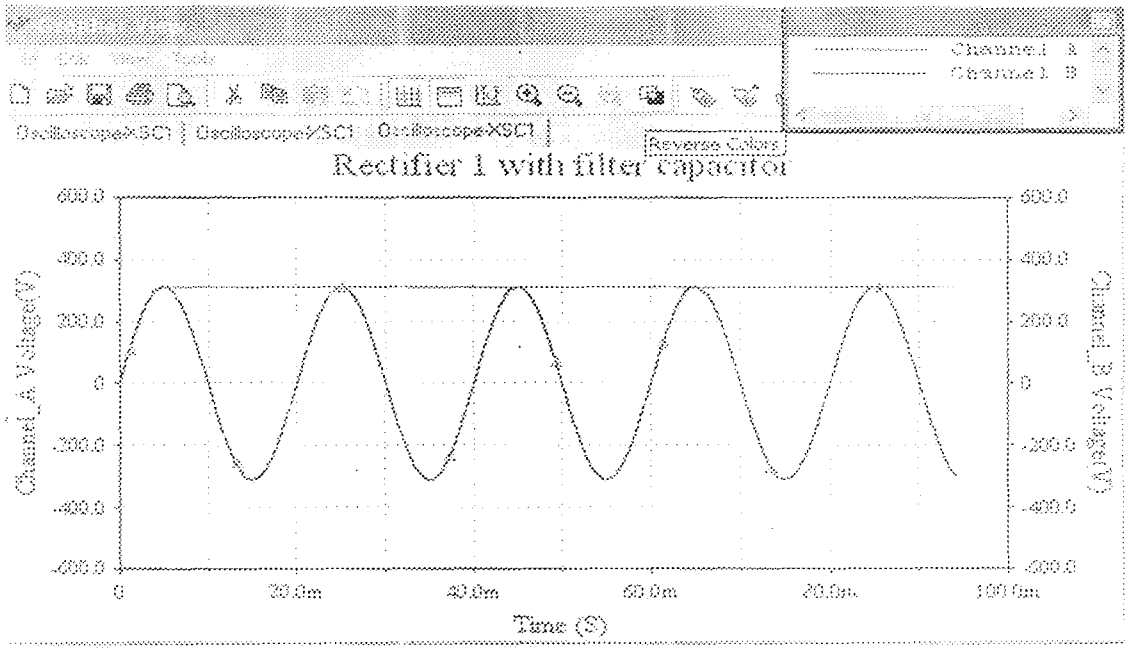

Figure 4.3: Simulated result obtained for Rectifier 1 with filter capacitor.

4.4 RECTIFIER 2 WITH FIXED REGULATOR OF LM7809

Figure 4.5 and 4.6 show the simulation layout for rectifier 2 that powers the control IC (ICSG3524).

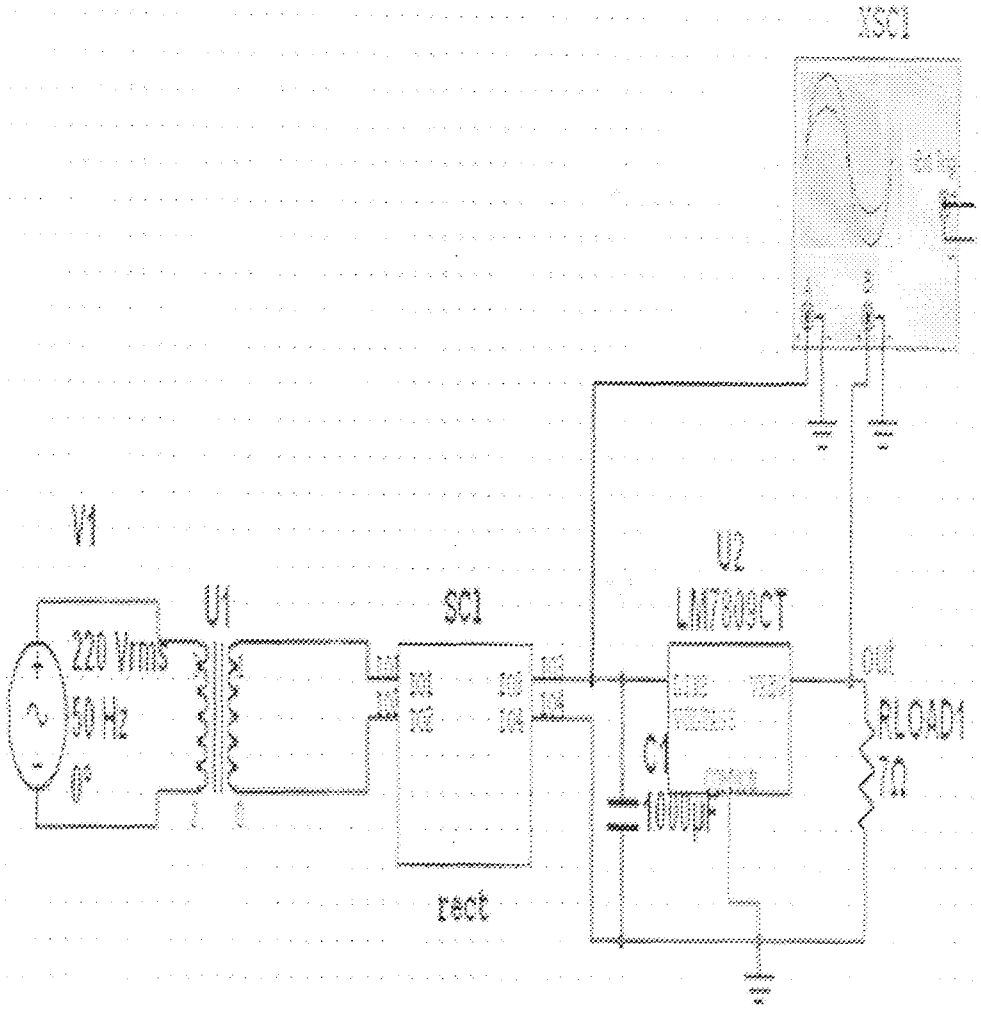

Figure 4.4: Rectifier 2 with a regulator output LM7809.

4.4.1 RECTIFIER 2 WITH OSCILLOSCOPE WAVEFORM OUTPUT

Figure 4.6 shows the simulation result obtained at the output of LM7809 The DC output signal was designated with red colour, while the AC sinusoidal was designated with blue colour.

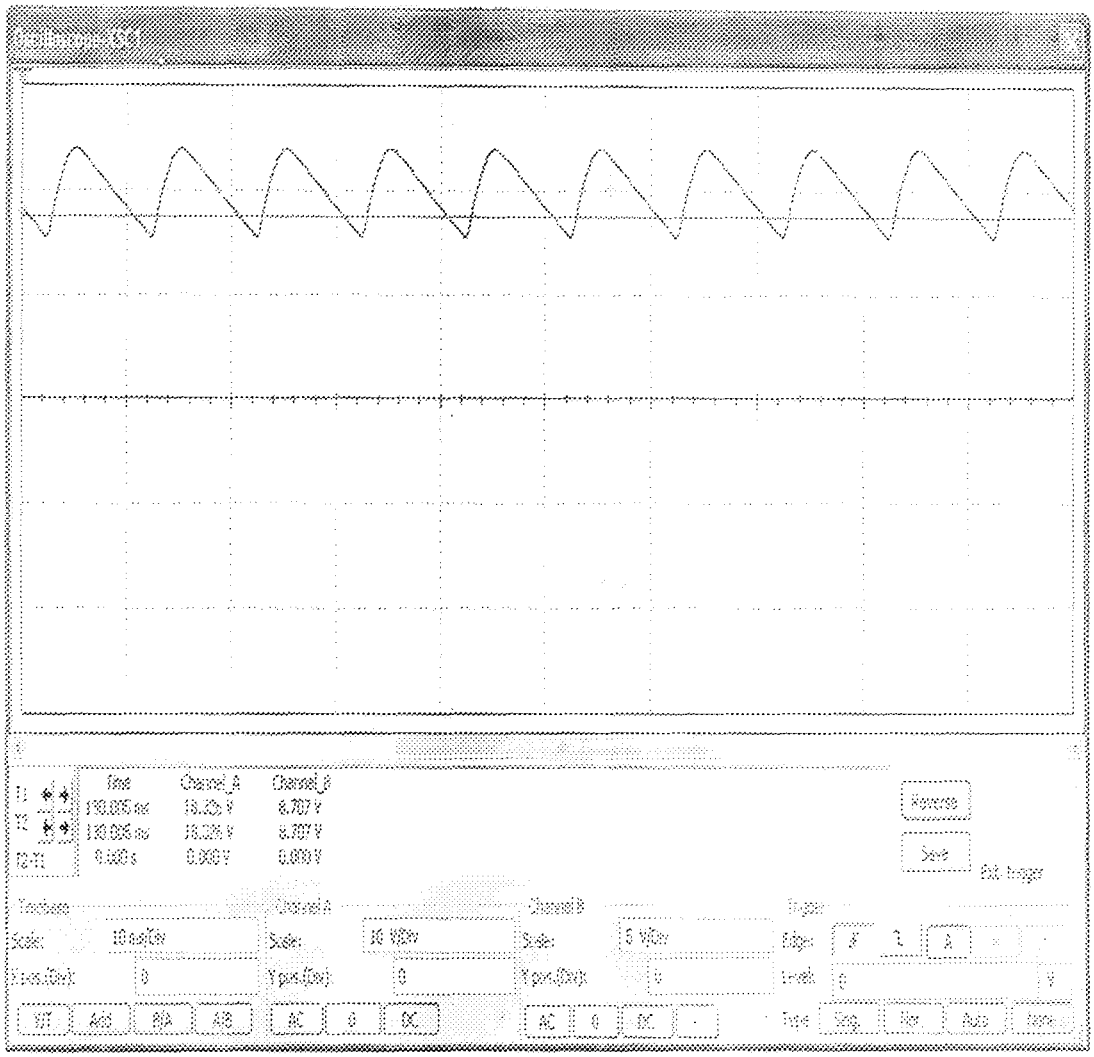

Figure 4.5: Rectifier 2 with a LM7809 regulator output simulated result, the red line shows the dc output from regulator, while the blue line shows unregulated ac.

4.5 COMPLETE CIRCUIT SIMULATION

Figure 4.7 shows the simulation achieved using Multism 10 for the entire circuit, while figure 4.8 shows the simulation output of 41.643V to charge the 36V battery.

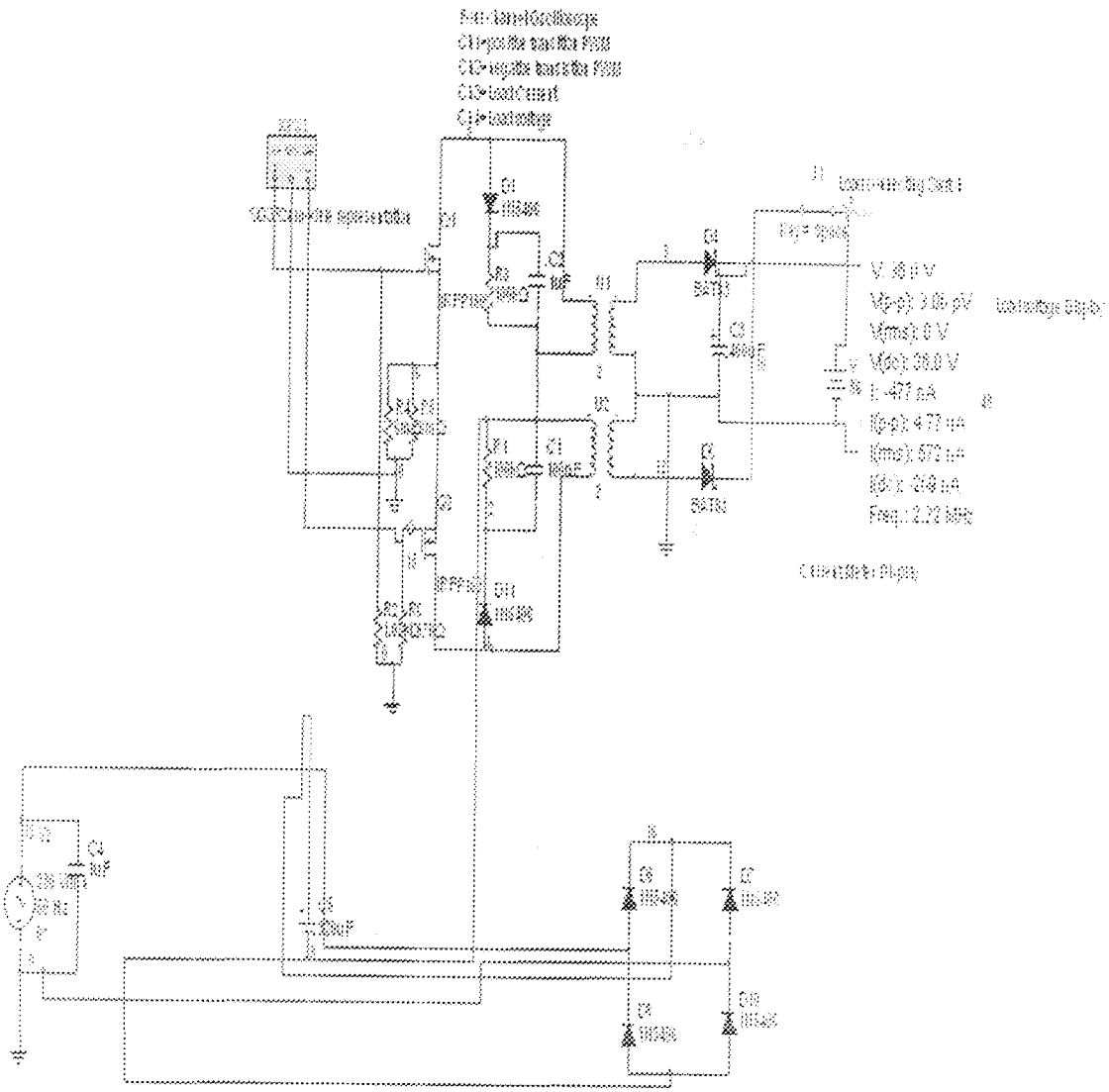

Figure 4.6: Showing simulation 1 of the entire circuit with Multism NI 10

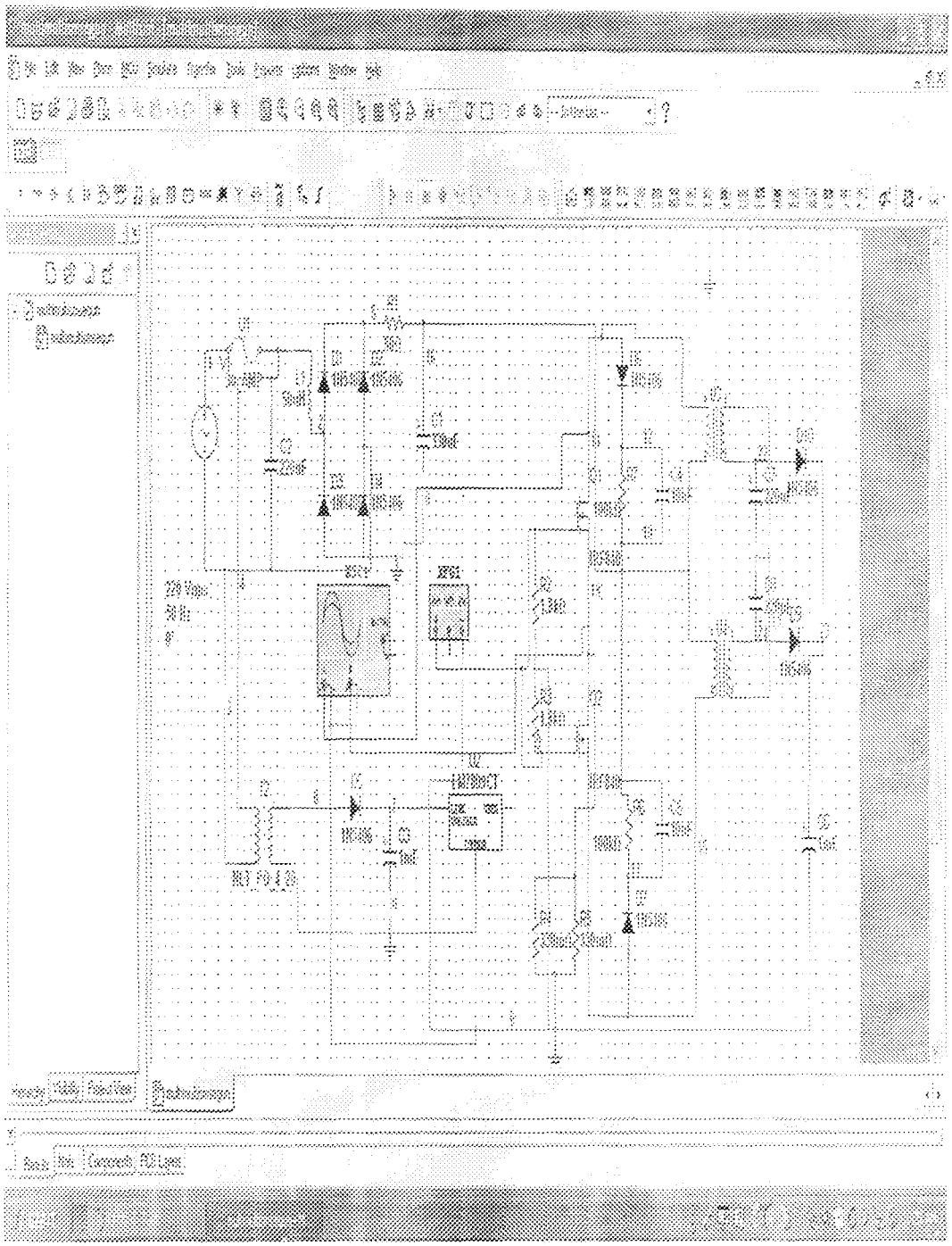

Figure 4.7: Showing simulation 2 of the entire circuit with Multisim NI 10

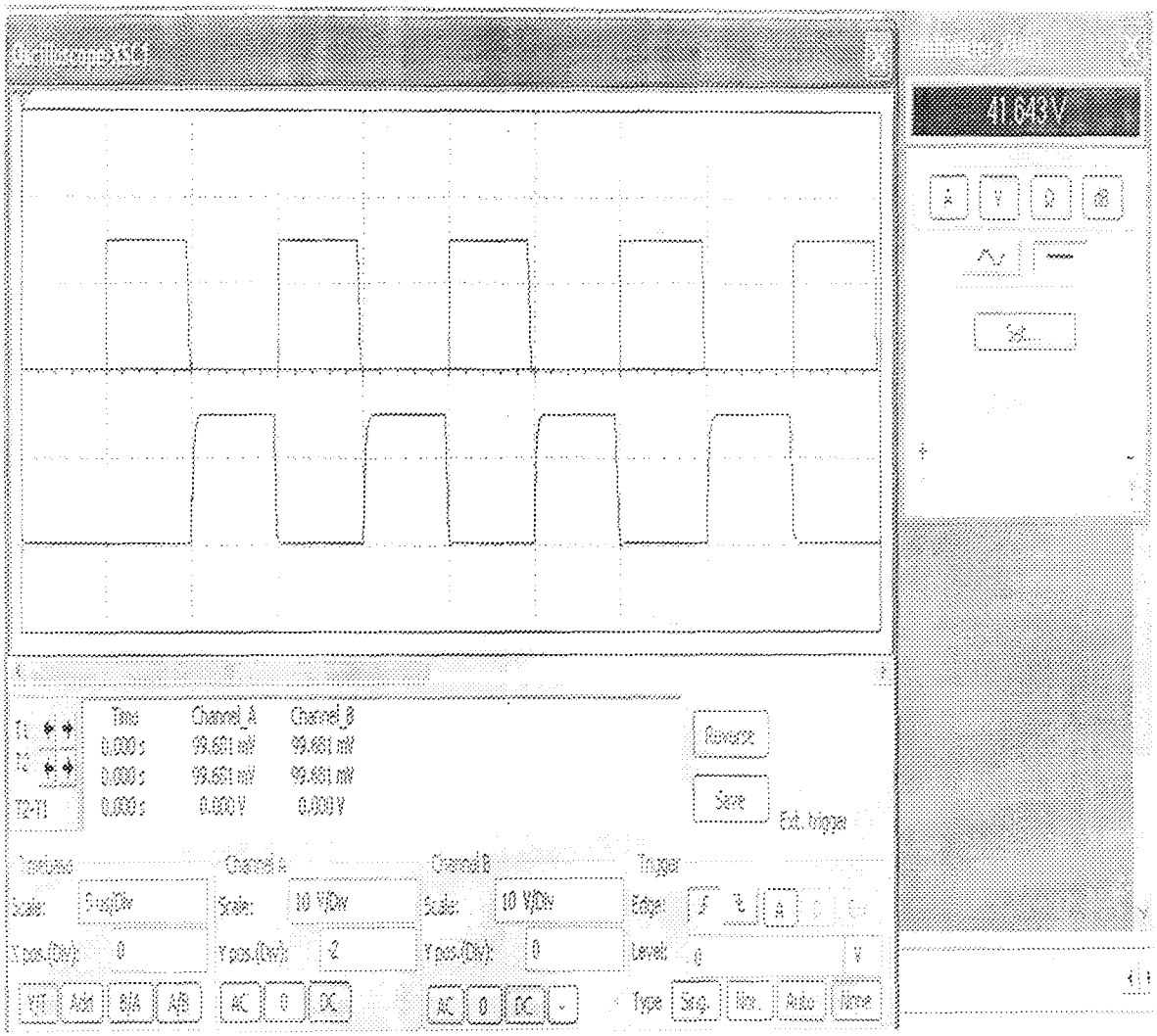

Figure 4.8: Showing simulation result of the PWM during T_{on} and T_{off}.

4.6 RESULTS OBTAINED

The following table 4.2 shows the results obtained when three 12V, 60A/hr discharged batteries were charged for 10 hours.

Table 4.1: Test results obtained when three batteries were observed

	Battery 1		Battery 2		Battery 3	
	Make: (Bosch)		Make: (Votak)		Make: (Spark)	
Battery	Discharged voltage	Charge voltage	Discharge	Charge	Discharge	Charge
1	12.15	13.62	11.88	13.61	11.58	13.63
2	12.15	13.64	11.92	13.6	11.61	13.63
3	12.13	13.64	11.87	13.57	12.17	13.61

4.7 PROJECT COST ESTIMATE

The total cost estimate for the project is Five Thousand and Ten naira only, which is cheaper than the market value for a linear charger. The total cost per component is attached in appendix 6 and 6A.

4.8 RELIABILITY ASSESSMENT OF THE BATTERY CHARGER

The battery charger reliability test R, was carried out for 8hours, with assumption of a continuous use for 365 days in a year using the expression

$$R = e^{-\lambda t} \qquad 4.1$$

Where R = Reliability

λ = System failure rate

t = Total operating time.

The weighting factors (Oroge)

Environments (all components), Wg	2.0
Temperature (all components), Wp	1.5
Rating, W_R	
Capacitors	3.0
Resistors	2.0
Transistors	2.0
Diodes	1.0

Table 4.2: Components and basic failure rate

COMPONENT	N= Number Used (n_i)	Basic Failure Rate, λ (%, 10^3hr.)	Weighting Factors due to			Overall Failure Rate $\lambda_p = \sum n_i \lambda_i . W_E . W_T . W_R$ (%/10^3 hr)
			Environments W_E	Temperature W_T	Rating W_R	
Electrolytic Capacitors	3	0.04	2.0	1.5	3.0	1.08
Fixed Capacitors	7	0.01	2.0	1.5	3.0	0.63
Variable Resistors	3	0.6	2.0	1.5	2.0	10.8
Thermistor	1	0.01	2.0	1.5	2.0	0.06
Transformer	1	0.01	2.0	1.5	1.0	0.03
Pulse Transformer	1	0.01	2.0	1.5	1.0	0.06
Zener diodes	5	0.01	2.0	1.5	1.5	0.225
Diodes	10	0.08	2.0	1.5	1.5	3.6
Voltmeter	1	0.01	2.0	1.5	1.5	0.045
Rectifier	1	0.2	2.0	1.5	2.0	1.2
Resistors	17	0.005	2.0	1.5	2.0	0.51
IC SG3524	1	0.01	2.0	1.5	2.0	0.06
MOSFET	2	0.05	2.0	1.5	2.0	0.6
TOTAL λ_T						18.9% /10^3 Hrs

From table 4.2, summation of all components failure rate will give the system failure rate.

$$\lambda_T = \sum \lambda_{0i} = 18.9\%/10^3 hr. \qquad 4.2$$

$$\lambda_T = 0.189/10^3 hr.$$

Total operating time, t = 8 x 365 = 2920 hours

From equation 4.1, the system reliability, R is determine

$$R = e^{-\lambda t}$$

$$R = e^{-0.189 \times 10^{-3} \times 2920}$$

$$R = e^{-0.5518}$$

$$R = 0.576$$

$$R \approx 0.6$$

From the result obtained as 0.6, it clearly indicate that the system is reliable since the value of R is greater than 0.5.

4.9 DURABILITY AND SAFETY OF THE BATTERY CHARGER

The use of accurate maximum duty cycle setting to stop charging responsible for the safety and durability of the charger. Also the use of heat sink with protective casing.

Finally the battery charger was connected across the three discharged 12V batteries in series, since a single 36V battery is not commercially available in the market now. The three batteries were charged for eight hours and an average value of 13.6V was the result obtained at the terminal of each of the three 12V battery, that confirm that the smps battery charger was okay.

CHAPTER FIVE

5.0 CONCLUSION AND RECOMMENDATIONS

5.1 CONCLUSION

The aim of this thesis was to demonstrate the implementation of the "42V battery charger". After a brief overview of the background information, design of the charger was carried out.

The 210W, 42V off board battery charger was subsequently built and tested with three batteries connected in series. The converter functioned as designed. The final product was able to regulate to 41.643V_{DC}. The charger showed excellent line and load regulation.

5.2 RECOMMENDATION

A new SMPS 42V charger for charging 36V battery to meet the need of modern vehicles was designed and built.

The successful implementation of the "42V battery charger" using half bridge push pull topology demonstrated in this thesis has shown promising results, and should provide an excellent platform for the development of higher power applications in vehicles in the near future.

REFERENCES

Ahmed, F. (2006). Modelling and Fault Diagnosis of Automotive Lead-Acid Batteries. Publication by Automotive Inc Germany, pp 8-12.

Andy, M. G. (1991). The development of a 100 KHZ switched-mode power supply. A thesis and dissertation by Cape Peninsula University of Technology, pp8-11; 67-70.

Brown, M. (2009). Efficient Switch Mode Power Supply Design with Minimum Components for 5W Output Power, Journal of Electrical Engineering & Technology, Vo l. 4, No.1, pp. 79~86.

Bhim, S and Ganesh, D. C. (2009). Efficient Switch Mode Power Supply Design with Minimum Components for 5W Output Power, Journal of Electrical Engineering & Technology, Vo l. 5, No.1, pp. 80~85.

Ceuca, I.E. (2005). Efficient Theoretical and Experimental Research in simulation of automotive power electronics circuits. Abstract of the PhD Thesis Technical University of Cluj-Napoca,Faculty of Electronics and Telecommunications.

Consoli A, Cacciato M, Scarcella G. (2004). A Multiphase Dc/Dc Converter For Automotive Dual-Voltage Power Systems. IEEE Industry Applications Magazine. Nov/Dec. 2004 pp 35-42.

Dell, A. C, Jr. and Gary L. (2000) .Batteries for 42/14 Volt Automotive Electrical Systems", Journal of Society of Automotive Engineers, Inc, Vol. 00FTT-61, pp. 1-6.

ECEN, Lecture note (2004) on lead-acid batteries ECEN4517/5517, pp19.

EG&G, Technical Services Inc, (2004) "Fuel Cell Handbook" U.S. Department of Energy Office of Fossil Energy National Energy Technology Laboratory, Morgantown, West Virginia 26507-0880, pp 67 & 275.

Ondrej, P. (1997). Low Cost 1.0A Current Source for Battery Chargers, Paper presentation by Industrial System Application Laboratory Motorola Product, Application note 1393, pp 1-7.

Oroge, C, O. (1991). Fundamentals of Reliability and Testing Methods, pp 28-29.Kaduna, Nigeria: Sooji Press.

Ilan , E.C. (2005). Theoretical and Experimental Research in simulation of automotive power electronics circuits. Research work of Tech. University of Cluj –

Napoces, pp. 1-7.

Ioan . W.H. (2001). Multilevel converter 42V dc to 14Vdc. Bachelor of Science Thesis in Electrical Engineering department at the University of Queensland, pp. 31-32.

Martin Hadartz and Martin Julander. (2008). Battery-Supercapacitor Energy Storage,a Master of Science Thesis in Electrical Engineering, Department of Energy and Environment, Division of Electric Power Engineering, Chalmers University Of Technology, Göteborg, Sweden, pp. 11-12.

McLyman, W.T, (2004). Transformer and Inductor Design Handbook, Idyllwild, California, U.S.A. pp. 126.

McLyman, W.T. (2004). Designing a Half Bridge Converter using a CoreMaster E2000Q Core Handbook, Application Note 108 pp.1-7.

Melissa, A.L. (2005). A versatile simulation tool for the design and verification of military vehicle power systems, paper presentation by Texas A & M University, pp. 112-113.

Mohammad A. (2004). Sliding Mode Control for Switched Mode Power Supplies, Ph.d. Thesis, Lappeenranta University of Technology Finland, pp. 13-14 & 18-20.

Mohammad. S. R. (2007). Buck Converter Design Issues. A master thesis, Linkoping electronic press, pp. 20, & 31-33.

Mohan N, Tore M. U, William P.R. (2003). Power Electronics Converters, Applications and Design, Third Edition, Wiley Technology and Engineering, pp. 301-360.

Nathan, R.T. (2002). X-by-Wire, New technologies for 42V Bus Automobile of the future South Carolina Honors College, pp.26.

Randyll. R. M. F, jr. (2005). Photovoltaic Power Converter For Military and Space Applications, M.Sc. Thesis, Naval Postgraduate School Monterey, California. Pp. 17-29.

Salvatore O, Diego.I and , Enrico.P. (2003). Control Strategy For Optimised Compound Set Of Supercaps and Electrochemical Batteries for Road Vehicles. Publication of University Of Napies Italy "Federico II", Department of Electrical Electronics Engineering, Vol. 7, No.2, December 2003. pp 80- 84.

Sagal K and Mohammed Kamil. (2009). Application note by microchip Technology (inc.),2355 West Chandler Chandler, AZ 8224-6199, AN1279, pp13-15.

Sangtaek, H. and Deepak .D. (2008). Directional DC/DC Converters for Plug-in Hybrid Electric Vehicle (PHEV) Applications.School of Electrical and Computer Engineering, Georgia Institute of Technology 777 Atlantic Dr. Atlanta GA, 30332 USA, pp.784-789.

Sheldon S. W. (2011). Lecture note on 439/6471Electric/Hybrid Electric Vehicle Power System Design and Control Department of Electrical and Computer Engineering, Concordia University De Maisonneuve West, Montreal, Quebec, pp. 36-38.

ST, Microelectronics Lecture note. (1999). Application Note on Topologies for Switched Mode Power Supplies. ST Microelectronics, pp. 14- 15.

Thorsten, G, and Carsten P. (2006). Analysis of Vehicle Power Supply Systems Using System Simulation, SAE Technical Paper Series, pp.1-9.

APPENDIX I: DESIGN AND DIMENSIONAL DATA FOR ETD, FERRITE CORES

Design and Dimensional Data for ETD, Ferrite Cores

The dimensional outline for ETD ferrite cores is shown in Figure 3-33. Dimensional data for ETD ferrite cores is given in Table 3-24; design data is given in Table 3-25.

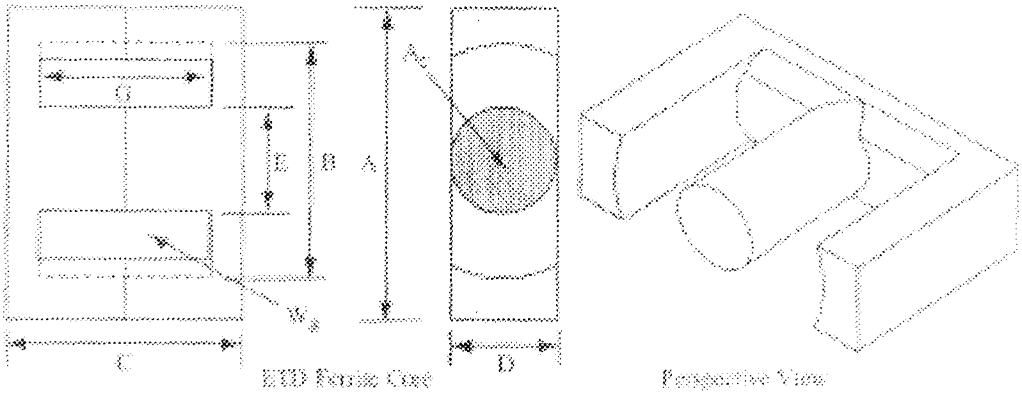

Figure 3-33. Dimension Outline for ETD Ferrite Cores.

Table 3-24. Dimensional Data for ETD Ferrite Cores.

ETD, Ferrite Cores (Ferroxcube)													
Part No.	A cm	B cm	C cm	D cm	E cm	G cm	Part No.	A cm	B cm	C cm	D cm	E cm	G cm
ETD-29	3.060	2.270	3.160	0.980	0.980	2.200	ETD-49	4.980	3.610	4.940	1.670	1.670	3.540
ETD-34	3.500	2.560	3.460	1.110	1.110	2.360	ETD-54	5.450	4.120	5.520	1.890	1.890	4.040
ETD-39	4.000	2.930	3.960	1.280	1.280	2.840	ETD-59	5.980	4.470	6.200	2.165	2.165	4.500
ETD-44	4.500	3.250	4.460	1.520	1.520	3.220							

Table 3-25. Design Data for ETD Ferrite Cores.

ETD, Ferrite Cores (Ferroxcube)											
Part No.	W_{tcu} grams	W_{tfe} grams	MLT cm	MPL cm	$\frac{W_a}{A_c}$	A_c cm^2	W_a cm^2	A_p cm^4	K_g cm^5	A_t cm^2	*AL mh/1K
ETD-29	32.1	28.0	6.4	7.20	1.865	0.761	1.419	1.0800	0.0517	42.5	1000
ETD-34	43.4	40.0	7.1	7.87	1.757	0.974	1.711	1.6665	0.0911	53.4	1182
ETD-39	69.3	60.0	8.3	9.22	1.871	1.252	2.343	2.9330	0.1766	69.9	1318
ETD-44	93.2	94.0	9.4	10.30	1.599	1.742	2.785	4.8520	0.3595	87.9	1682
ETD-49	126.2	124.0	10.3	11.40	1.627	2.110	3.434	7.2453	0.5917	107.9	1909
ETD-54	186.9	180.0	11.7	12.70	1.609	2.800	4.505	12.6129	1.2104	131.7	2273
ETD-59	237.7	260.0	12.9	13.90	1.410	3.677	5.186	19.0698	2.1271	163.1	2727

*This AL value has been normalized for a permeability of 1K. For a close approximation of AL for other values of permeability, multiply this AL value by the new permeability in kilo-perm. If the new permeability is 2500, then use 2.5.

APPENDIX 2: SINGLE CORE PVC WIRING CABLE (NCV)

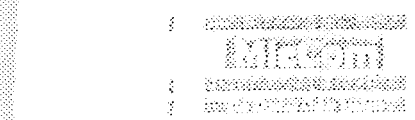

SINGLE CORE PVC WIRING CABLE (NCV)

NOMINAL CROSS SECTIONAL AREA mm²	CONDUCTOR NUMBER AND DIAMETER OF WIRE (mm) ROUND	NOMINAL OVERALL DIAMETER (mm)	MAXIMUM CURRENT RATING Amp		STANDARD DELIVERY LENGTH (METRES)
			IN PIPE	IN AIR	
1	1/1.13	2.3	10	16	100
1.5	1/1.38	2.8	13	21	100
2.5	1/1.78	3.3	17	28	100
4	1/2.25	3.9	22	37	100
6	1/2.76	4.4	29	48	100
10	7/1.35	6.1	39	64	100
16	7/1.70	7.1	53	86	100
25	7/2.14	9.0	72	112	100
35	7/2.50	9.9	90	138	100
50	19/1.78	11.7	115	172	100
70	19/2.14	13.5	144	213	100
95	19/2.52	15.9	172	254	100
120	19/2.85	17.4	205	300	100
150	37/2.25	19.4	0	340	100
185	19/2.52	21.6	0	390	100
240	37/2.85	24.7	0	460	100
300	37/3.20	27.6	0	530	100
400	61/2.85	30.9	0	634	100
500	61/3.20	34.4	0	722	100
630	91/2.98	38.3	0	970	100

APPENDIX 3 SHOWING MATLAB CODE PROGRAM FOR SOLVING EQUATION 3.10 TO 3.12C

```
% Single phase Diode rectifier bridge
R = 1000; %set the value of R and C as 1k and 1uf
C = 1e-6; ampl=191;
f=50;
w=2*pi*f;
t = 0:0.0001:0.05; %t is a vector from 0 to .01 in steps of .0001
%use vector operations to find vc and ic and es.
es=ampl*sin(w*t);
vc = ampl*(1-exp(-t/(R*C)));
ic = ampl*exp(-t/(R*C));
x=[vc;ic]
plot(t,es,'blue',t,vc,'red',t,ic,'green')
title('Capacitor voltage, capacitor current and source voltage'); %Create a title for this
graph
xlabel('Time'); %label the x axis
ylabel('Volts and milliamps'); %label the y axis
figure(2);clf; %A second figure for the voltage
plot(t,vc,'red',t,ic,'green')
title('Capacitor voltage and capacitor current'); %Create a title for this graph
xlabel('Time'); %label the x axis
ylabel('Volts and milliamps'); %label the y axis
figure(3);clf; %A second figure for the voltage
plot(t, vc); %plot time vs capacitor voltage
title('Capacitor voltage'); %Create a title for this graph
xlabel('Time'); %label the x axis
ylabel('Volts'); %label the y axis
figure(4);clf; %A second figure for the current
plot(t, ic); %plot time vs capacitor current on figure 2
title('Capacitor current'); %add titles and axis labels.
xlabel('Time'); ylabel('milliamps');
```

APPENDIX 4 MATLAB CODE RESULT OBTAINED FOR SOLVING EQUATION 3.10 TO 3.12C

x = Columns 1 through 15

0 18.1761 34.6224 49.5037 62.9689 75.1526 86.1770 96.1522 105.1782 113.3452 120.7350 127.4216 133.4719 138.9464 143.9000

191.0000 172.8239 156.3776 141.4963 128.0311 115.8474 104.8230 94.8478 85.8218 77.6548 70.2650 63.5784 57.5281 52.0536 47.1000

Columns 16 through 30

148.3821 152.4378 156.1074 159.4279 162.4324 165.1510 167.6108 169.8366 171.8506 173.6729 175.3218 176.8137 178.1637 179.3853 180.4906

42.6179 38.5622 34.8926 31.5721 28.5676 25.8490 23.3892 21.1634 19.1494 17.3271 15.6782 14.1863 12.8363 11.6147 10.5094

Columns 31 through 45

181.4907 182.3956 183.2144 183.9553 184.6257 185.2323 185.7812 186.2778 186.7272 187.1338 187.5017 187.8346 188.1358 188.4084 188.6550

9.5093 8.6044 7.7856 7.0447 6.3743 5.7677 5.2188 4.7222 4.2728 3.8662 3.4983 3.1654 2.8642 2.5916 2.3450

Columns 46 through 60

188.8782 189.0801 189.2628 189.4281 189.5777 189.7131 189.8355 189.9463 190.0466 190.1373 190.2194 190.2937 190.3609 190.4217 190.4768

2.1218 1.9199 1.7372 1.5719 1.4223 1.2869 1.1645 1.0537 0.9534 0.8627 0.7806 0.7063 0.6391 0.5783 0.5232

Columns 61 through 75

190.5266 190.5716 190.6124 190.6493 190.6826 190.7128 190.7402 190.7649 190.7873 190.8075 190.8258 190.8424 190.8574 190.8710 190.8833

0.4734 0.4284 0.3876 0.3507 0.3174 0.2872 0.2598 0.2351 0.2127 0.1925 0.1742 0.1576 0.1426 0.1290 0.1167

Columns 76 through 90

190.8944 190.9044 190.9135 190.9217 190.9292 190.9359 190.9420 190.9475 190.9525 190.9571 190.9611 190.9648 190.9682 190.9712 190.9739

0.1056 0.0956 0.0865 0.0783 0.0708 0.0641 0.0580 0.0525 0.0475 0.0429 0.0389 0.0352 0.0318 0.0288 0.0261

Columns 91 through 105

190.9764 190.9787 190.9807 190.9825 190.9842 190.9857 190.9871 190.9883 190.9894 190.9904 190.9913 190.9922 190.9929 190.9936 190.9942

0.0236 0.0213 0.0193 0.0175 0.0158 0.0143 0.0129 0.0117 0.0106 0.0096 0.0087 0.0078 0.0071 0.0064 0.0058

Columns 106 through 120

190.9947 190.9952 190.9957 190.9961 190.9965 190.9968 190.9971 190.9974 190.9976 190.9979 190.9981 190.9982 190.9984 190.9986 190.9987

0.0053 0.0048 0.0043 0.0039 0.0035 0.0032 0.0029 0.0026 0.0024 0.0021 0.0019 0.0018 0.0016 0.0014 0.0013

Columns 121 through 135

190.9988 190.9989 190.9990 190.9991 190.9992 190.9993 190.9994 190.9994 190.9995 190.9995 190.9996 190.9996 190.9996 190.9997 190.9997

0.0012 0.0011 0.0010 0.0009 0.0008 0.0007 0.0006 0.0006 0.0005 0.0005 0.0004 0.0004 0.0004 0.0003 0.0003

Columns 136 through 150

190.9997 190.9998 190.9998 190.9998 190.9998 190.9998 190.9999 190.9999 190.9999 190.9999 190.9999 190.9999 190.9999 190.9999 190.9999

0.0003 0.0002 0.0002 0.0002 0.0002 0.0002 0.0001 0.0001 0.0001 0.0001 0.0001 0.0001 0.0001 0.0001 0.0001

Columns 151 through 165

190.9999 190.9999 191.0000 191.0000 191.0000 191.0000 191.0000 191.0000 191.0000 191.0000 191.0000 191.0000 191.0000 191.0000 191.0000

0.0001 0.0001 0.0000 0.0000 0.0000 0.0000 0.0000 0.0000 0.0000 0.0000 0.0000 0.0000 0.0000 0.0000 0.0000

Columns 166 through 180

191.0000 191.0000 191.0000 191.0000 191.0000 191.0000 191.0000 191.0000 191.0000 191.0000 191.0000 191.0000 191.0000 191.0000 191.0000

0.0000 0.0000 0.0000 0.0000 0.0000 0.0000 0.0000 0.0000 0.0000 0.0000 0.0000 0.0000 0.0000 0.0000 0.0000

Columns 181 through 195

191.0000 191.0000 191.0000 191.0000 191.0000 191.0000 191.0000 191.0000 191.0000 191.0000 191.0000 191.0000 191.0000 191.0000 191.0000

0.0000 0.0000 0.0000 0.0000 0.0000 0.0000 0.0000 0.0000 0.0000 0.0000 0.0000 0.0000 0.0000 0.0000 0.0000

Columns 196 through 210

191.0000 191.0000 191.0000 191.0000 191.0000 191.0000 191.0000 191.0000 191.0000 191.0000 191.0000 191.0000 191.0000 191.0000 191.0000

0.0000 0.0000 0.0000 0.0000 0.0000 0.0000 0.0000 0.0000 0.0000 0.0000 0.0000 0.0000 0.0000 0.0000 0.0000

Columns 211 through 225

191.0000 191.0000 191.0000 191.0000 191.0000 191.0000 191.0000 191.0000 191.0000 191.0000 191.0000 191.0000 191.0000 191.0000 191.0000

0.0000 0.0000 0.0000 0.0000 0.0000 0.0000 0.0000 0.0000 0.0000 0.0000 0.0000 0.0000 0.0000 0.0000 0.0000

Columns 226 through 240

191.0000 191.0000 191.0000 191.0000 191.0000 191.0000 191.0000 191.0000 191.0000 191.0000 191.0000 191.0000 191.0000 191.0000 191.0000

0.0000 0.0000 0.0000 0.0000 0.0000 0.0000 0.0000 0.0000 0.0000 0.0000 0.0000 0.0000 0.0000 0.0000 0.0000

Columns 241 through 255

191.0000 191.0000 191.0000 191.0000 191.0000 191.0000 191.0000 191.0000 191.0000 191.0000 191.0000 191.0000 191.0000 191.0000 191.0000

0.0000 0.0000 0.0000 0.0000 0.0000 0.0000 0.0000 0.0000 0.0000 0.0000 0.0000 0.0000 0.0000 0.0000 0.0000

Columns 256 through 270

191.0000 191.0000 191.0000 191.0000 191.0000 191.0000 191.0000 191.0000 191.0000 191.0000 191.0000 191.0000 191.0000 191.0000 191.0000

0.0000 0.0000 0.0000 0.0000 0.0000 0.0000 0.0000 0.0000 0.0000 0.0000 0.0000 0.0000 0.0000 0.0000 0.0000

Columns 271 through 285

191.0000 191.0000 191.0000 191.0000 191.0000 191.0000 191.0000 191.0000 191.0000 191.0000 191.0000 191.0000 191.0000 191.0000 191.0000

0.0000 0.0000 0.0000 0.0000 0.0000 0.0000 0.0000 0.0000 0.0000 0.0000 0.0000 0.0000 0.0000 0.0000 0.0000

Columns 286 through 300

191.0000 191.0000 191.0000 191.0000 191.0000 191.0000 191.0000 191.0000 191.0000 191.0000 191.0000 191.0000 191.0000 191.0000 191.0000

0.0000 0.0000 0.0000 0.0000 0.0000 0.0000 0.0000 0.0000 0.0000 0.0000 0.0000 0.0000 0.0000 0.0000 0.0000

Columns 301 through 315

191.0000 191.0000 191.0000 191.0000 191.0000 191.0000 191.0000 191.0000 191.0000 191.0000 191.0000 191.0000 191.0000 191.0000 191.0000

0.0000 0.0000 0.0000 0.0000 0.0000 0.0000 0.0000 0.0000 0.0000 0.0000 0.0000 0.0000 0.0000 0.0000 0.0000

Columns 316 through 330

191.0000 191.0000 191.0000 191.0000 191.0000 191.0000 191.0000 191.0000 191.0000 191.0000 191.0000 191.0000 191.0000 191.0000 191.0000

0.0000 0.0000 0.0000 0.0000 0.0000 0.0000 0.0000 0.0000 0.0000 0.0000 0.0000 0.0000 0.0000 0.0000 0.0000

Columns 331 through 345

191.0000 191.0000 191.0000 191.0000 191.0000 191.0000 191.0000 191.0000 191.0000 191.0000 191.0000 191.0000 191.0000 191.0000 191.0000

0.0000 0.0000 0.0000 0.0000 0.0000 0.0000 0.0000 0.0000 0.0000 0.0000 0.0000 0.0000 0.0000 0.0000 0.0000

Columns 346 through 360

191.0000 191.0000 191.0000 191.0000 191.0000 191.0000 191.0000 191.0000 191.0000 191.0000 191.0000 191.0000 191.0000 191.0000 191.0000

0.0000 0.0000 0.0000 0.0000 0.0000 0.0000 0.0000 0.0000 0.0000 0.0000 0.0000 0.0000 0.0000 0.0000 0.0000

Columns 361 through 375

191.0000 191.0000 191.0000 191.0000 191.0000 191.0000 191.0000 191.0000 191.0000 191.0000 191.0000 191.0000 191.0000 191.0000 191.0000

0.0000 0.0000 0.0000 0.0000 0.0000 0.0000 0.0000 0.0000 0.0000 0.0000 0.0000 0.0000 0.0000 0.0000 0.0000

Columns 376 through 390

191.0000 191.0000 191.0000 191.0000 191.0000 191.0000 191.0000 191.0000 191.0000 191.0000 191.0000 191.0000 191.0000 191.0000 191.0000

0.0000 0.0000 0.0000 0.0000 0.0000 0.0000 0.0000 0.0000 0.0000 0.0000 0.0000 0.0000 0.0000 0.0000 0.0000

Columns 391 through 405

191.0000 191.0000 191.0000 191.0000 191.0000 191.0000 191.0000 191.0000 191.0000 191.0000 191.0000 191.0000 191.0000 191.0000 191.0000

0.0000 0.0000 0.0000 0.0000 0.0000 0.0000 0.0000 0.0000 0.0000 0.0000 0.0000 0.0000 0.0000 0.0000 0.0000

Columns 406 through 420

191.0000 191.0000 191.0000 191.0000 191.0000 191.0000 191.0000 191.0000 191.0000 191.0000 191.0000 191.0000 191.0000 191.0000 191.0000

0.0000 0.0000 0.0000 0.0000 0.0000 0.0000 0.0000 0.0000 0.0000 0.0000 0.0000 0.0000 0.0000 0.0000 0.0000

Columns 421 through 435

191.0000 191.0000 191.0000 191.0000 191.0000 191.0000 191.0000 191.0000 191.0000 191.0000 191.0000 191.0000 191.0000 191.0000 191.0000

0.0000 0.0000 0.0000 0.0000 0.0000 0.0000 0.0000 0.0000 0.0000 0.0000 0.0000 0.0000 0.0000 0.0000 0.0000

Columns 436 through 450

191.0000 191.0000 191.0000 191.0000 191.0000 191.0000 191.0000 191.0000 191.0000 191.0000 191.0000 191.0000 191.0000 191.0000 191.0000

0.0000 0.0000 0.0000 0.0000 0.0000 0.0000 0.0000 0.0000 0.0000 0.0000 0.0000 0.0000 0.0000 0.0000 0.0000

Columns 451 through 465

191.0000 191.0000 191.0000 191.0000 191.0000 191.0000 191.0000 191.0000 191.0000 191.0000 191.0000 191.0000 191.0000 191.0000 191.0000

0.0000 0.0000 0.0000 0.0000 0.0000 0.0000 0.0000 0.0000 0.0000 0.0000 0.0000 0.0000 0.0000 0.0000 0.0000

Columns 466 through 480

191.0000 191.0000 191.0000 191.0000 191.0000 191.0000 191.0000 191.0000 191.0000 191.0000 191.0000 191.0000 191.0000 191.0000 191.0000

0.0000 0.0000 0.0000 0.0000 0.0000 0.0000 0.0000 0.0000 0.0000 0.0000 0.0000 0.0000 0.0000 0.0000 0.0000

Columns 481 through 495

191.0000 191.0000 191.0000 191.0000 191.0000 191.0000 191.0000 191.0000 191.0000 191.0000 191.0000 191.0000 191.0000 191.0000 191.0000

0.0000 0.0000 0.0000 0.0000 0.0000 0.0000 0.0000 0.0000 0.0000 0.0000 0.0000 0.0000 0.0000 0.0000 0.0000

Columns 496 through 501

191.0000 191.0000 191.0000 191.0000 191.0000 191.0000

0.0000 0.0000 0.0000 0.0000 0.0000 0.0000

APPENDIX 5 SHOWING LIST OF COMPONENTS USED

Designation	Value/Rating
C2	330µF, 400V
C3	10µF, 15V
C4	10,000µF, 50V
C5, C6	103µF, 1KV
C7	10nF, 103k
C8	104µF
C9, C10	0.33K
D1 - D4	IN5406
D5 – D7	IN4148
D8 – D9	IN4007
D10 – D12	IN4007
L1	10nH
L2	10nH
Q1, Q2	IRF460
R1	100K
R2	5.6K
R3	10K
R4	100K
R5	27Ω
R2, R6, R7	100K
R7, R8, R9	470Ω
R10	33K

APPENDIX 5A SHOWING LIST OF COMPONENTS USED

Designation	Value/Rating
R11	1K
R12	20K
R13, R14	0.33Ω
R15, R16	1.8K
Transformer number of turns	$N_P = 12$, $N_S = 3$
U1	IC – SG3524

APPENDIX 6 SHOWING PROJECT COST ESTIMATE

Components	Cost (₦)

C2 = 330μF, 400V	350.00
C3 = 10μF, 15V	200.00
C4 = 10,000μF, 50V	150.00
C5, C6 = 103μF, 1KV	400.00
C7 = 10nF, 103k	200.00
C8 = 104μF	50.00
C9, C10 = 0.33K	120.00
D1 - D4 = IN5406	240.00
D5 – D7 = IN4148	100.00
D8 – D9 = IN4007	200.00
D10 – D12 = IN4007	120.00
L1 =10nH	40.00
L2 = 10mH	60.00
Q1, Q2 = IRF460	550.00
R1 =100K	20.00
R2 = 5.6K	35.00
R3 = 10K	35.00
R4 = 100K	80.00
R5 = 27Ω	20.00
R2, R6, R7 = 100K	60.00
R7, R8, R9 = 470Ω	60.00
R10 = 33K	20.00

APPENDIX 6A **SHOWING PROJECT COST ESTIMATE**

Components	Cost (₦)
R11 =1K	20.00
R12 = 20K	250.00
R13, R14 = 0.33Ω	40.00
R15, R16 = 1.8K	120.00
Transformer number of turns = N_P = 12, N_S = 3	450.00
U1 = IC – SG3524	350.00
Casing	500.00
Painting	200.00
TOTAL COST	**₦8010.00**